

# CONCEPTUAL DESIGN OF AN ORBITAL DEBRIS DEFENSE SYSTEM

West Virginia University  
Department of Mechanical and Aerospace Engineering  
Morgantown, West Virginia

*1N-18-CR*  
*2018/*  
*(41)*

Dr. Timothy L. Norman, Asst. Prof

Mr. David E Gaskin, NASA/USRA Grad TA

Mr. Erik Bedillion

Mr. Gary Blevins

Mr. Brian Bohs

Mr. David Bragg

Mr. Christopher Brown

Mr. Jose Casanova

Mr. David Cribbs

Mr. Richard Demko

Mr. Brian Henry

Ms. Kelly James

Ms. Kerri Knots

Ms. Stephanie Mayor

Mr. Scott Messick

Ms. Lori Minick

Mr. David Podnar

Mr. Tom Rankin

Mr. Jeff Rigglemen

Mr. Jeff Robinson

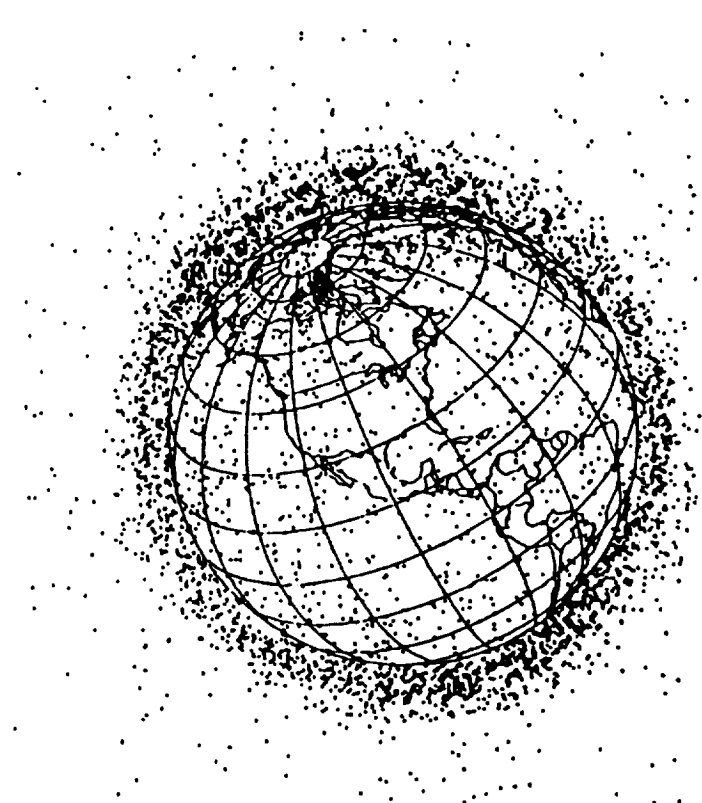
Mr. Enoch Ross

Ms. Jeannette Simmons

Mr. Taylor Strack

Mr. Tsuyoshi Kurosawa

Ms. Amy Yates



N95-12696

Unclas

G3/18 0026181

(NASA-CR-197211) CONCEPTUAL DESIGN  
OF AN ORBITAL DEBRIS DEFENSE SYSTEM  
(West Virginia Univ.) 64 p

## ACKNOWLEDGEMENTS

The MAE 236 design class would like to thank the following persons for their important contributions. Their help was vital to the completion of the design.

### I. NASA- George C. Marshall Space Flight Center

#### A. Program Development Office - Charles Darwin (Director)

##### 1. Preliminary Design Office

Frank Swalley Deputy Director WVU/MSFC Center Mentor

##### a. System Engineering Division

Bill Shelton Chief

Dianne Moe Secretary

##### 1. Structural & Thermal Analysis Branch

Bob Porter Chief

##### 2. All employees of Program Development

#### B. Marshall Scientific Library

#### C. Marshall Repository

### II. University Space Research Association - Advanced Design Program

Dr. Vicki Johnson

Ms. Kay Nute

Ms. Barabra Rumbaugh

Ms. Cissy Novak

Mr. John Sevier

Special thanks to Ms. Sue McCown

### III. NASA- Johnson Space Center

James E. Simpson

Eric Christensen

Navigation and Guidance Systems Branch

### IV. NSWC-White Oak MD

Dr. William T. Messick

### V. West Virginia University

#### A. Department of Mechanical and Aerospace Engineering

Dr. Timothy L. Norman Assistant Professor

Dr. Richard Walters Associate Chairman

Dr. Ever J. Barbero Assistant Professor

Dr. Alexi Leskin Assistant Professor

Dr. Gary Morris Associate Professor

## ABSTRACT

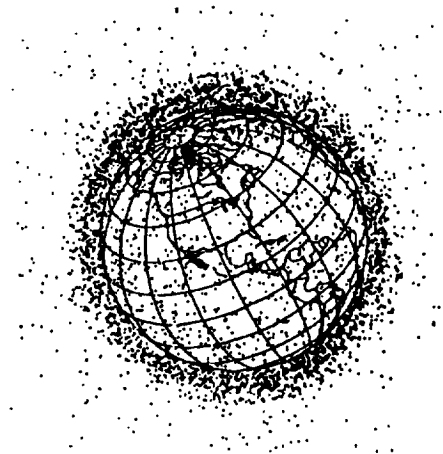
### CONCEPTUAL DESIGN OF AN ORBITAL DEBRIS DEFENSE SYSTEM

West Virginia University  
Department of Mechanical and Aerospace Engineering  
West Virginia University

Dr. Timothy L. Norman, Asst. Prof.  
David E. Gaskin, NASA/USRA Grad. TA

Man made orbital debris has become a serious problem. Currently NORAD tracks over 7000 objects in orbit and less than 10% of these are active payloads. Common estimates are that the amount of debris will increase at a rate of 10% per year. Impacts of space debris with operational payloads or vehicles is a serious risk to human safety and mission success. For example, the impact of a 0.2 mm diameter paint fleck with the Space Shuttle Challenger window created a 2 mm wide by 0.6 mm deep pit. The cost to replace the window was over \$50,000.

Twenty-three West Virginia University students conducted a conceptual design of an Orbital Debris Defense System (ODDS). The WVU design considered the wide range of debris sizes, orbits and velocities. Two vehicles were designed to collect and remove space debris. The first vehicle would attach a re-entry package to de-orbit very large debris, e.g. inactive satellites and spent upper stages that tend to break up and form small debris. This vehicle was designed to contain several re-entry packages, and be refueled and resupplied with more re-entry packages as needed. The second vehicle was designed to rendezvous with and capture debris ranging from 10 cm to 2 m. Due to tracking limitations, no technically feasible method for collecting debris below 10 cm in size could be devised; it must be accomplished through international regulations which reduce the accumulation of space debris.



## FOREWORD

Orbital debris is becoming a concern for all nations involved in space research and exploration. NORAD currently tracks over 7000 objects orbiting the Earth with a size of ten centimeters or larger. Less than five percent of these object, however, are active satellites. The remnants are considered orbital debris. There are also thought to be millions more smaller objects in orbit, too small to be detected from the ground.

The largest concentrations of satellite objects are located at inclinations of 20 to 30 degrees and 60 to 70 degrees. Orbits around 800, 1000, and 1500 kilometers contain the greatest concentration of objects. These are the altitudes and orbits used regularly for American space efforts. Geosynchronous orbit, where many communications and observation satellites are placed, has a growing population of objects, though it is evenly distributed around the planet.

Current estimates put the growth rate of orbital debris at 10% per year. Because of the possible complications of space operations in the future resulting from collisions or avoidance of space debris, it has been suggested by several agencies, including NASA and the AIAA, that a solution to the problem be studied now and implemented as soon as possible.

The students of West Virginia University NASA/USRA design class have taken on the goal of reducing the space debris problem. To this end, they have concentrated on designing an orbital debris defense system.

## TABLE OF CONTENTS

ACKNOWLEDGEMENTS	i
ABSTRACT	ii
FORWARD	iii
ACRONYMS	vi
SECTION A: SYSTEMS INTEGRATION	
A1. Problem Statement	A1
A2. Design Objectives	A1
A3. Executive Summary	A1
SECTION B: MEDIUM DEBRIS	
B1. Section Design Philosophy	B1
B2. Design Development	B1
B2.1 Passive Collection	B1
B2.2 Quick Response System	B2
B2.3 Impact Collector	B3
B2.4 Cutter/ Grinder System	B3
B3. Conceptual Design	B4
B3.1 Mission Scenario	B4
B3.2 Layout	B5
B3.3 Propulsion	B5
B3.4 Power Requirements	B6
B4. Conclusions	B6
SECTION C: LARGE DEBRIS	
C1. Design Philosophy	C1
C1.1 Definition of Problem	C1
C1.2 Background	C1
C1.3 Objective	C2
C2. Design Evolution and Development	C2
C2.1 Debris Collection Unit	C2
C2.2 Satellite Collection Unit	C4
C3. Deorbit Modular Vehicle (DMV)	C6
C3.1 Mission Scenario	C6
C3.2 Structural Description	C8
C3.3 Operational Components	C9
C3.3.1 Propulsion	C9
C3.3.2 Power	C9
C3.3.3 Guidance, Navigation and Control	C10
C3.3.4 Tracking	C11
C3.3.5 Resupply	C11
C3.3.6 Orbital Deployment	C11

C3.4 Capture Assembly	C11
C3.4.1 Spin Ring	C12
C3.4.2 Robotic Arm	C13
C3.4.3 End Effector	C13
C3.5 Deorbit Modules (DOM)	C15
C3.5.1 Attachment	C15
C3.5.2 Propulsion	C20
C4. Conclusions	C21
SECTION D: SHIELDING	
D1. Section Design Philosophy	D1
D2. Description of Shields	D1
D2.1 Basic Shields	D1
D2.2 Advanced Shields	D2
D3. Analysis of Shielding Technology	D3
D4. Results	D5
D4.1 Mesh Double Bumper	D5
D4.2 Multi-Shock	D6
D5. Conclusions	D7
SECTION E: DETECTION/TRACKING	
E1. Ground Based Tracking Systems	E1
E2. Large Debris Collection	E3
E3. Medium Debris Collection	E3
E4. Conclusions	E3
CONCLUSIONS	F1
RECOMMENDATIONS	F1
REFERENCES	F2

## ACRONYMS

CCD  
DMV  
DOM  
GEO  
GNC  
HIT-F  
JSC  
MDB  
MS  
ODDS  
OMV  
USSPACECOM

Charge Couple Device  
Deorbit Modular Vehicle  
Deorbit Module  
Geosynchronous Orbit  
Guidance Navigation Control  
Hypervelocity Impact Test Facility  
Johnson Space Center  
Mesh Double Bumper  
Multi Shock  
Orbital Debris Defense System  
Orbital Maneuvering Vehicle  
United States Space Command

## SECTION A: SYSTEM INTEGRATION

David Cribbs

**A1. Problem Statement.** Orbital debris is becoming a concern for all nations involved in space research and exploration. NORAD currently tracks over 7000 objects orbiting the Earth with a size of ten centimeters or larger<sup>A1</sup>. Less than five percent of these objects, however, are active satellites<sup>A2</sup>. The remnants are considered orbital debris. There are also thought to be millions more smaller objects in orbit, too small to be detected from the ground.

Current estimates put the growth rate of orbital debris at 10% per year<sup>A3</sup>. Because of the possible complications of space operations in the future resulting from collisions or avoidance of space debris, it has been suggested by several agencies, including NASA and the AIAA, that a solution to the problem be studied now and implemented as soon as possible<sup>A1</sup>.

**A2. Design Objectives.** The overall goal was to understand the space debris problem and potential solutions. Thus, the design objective was to perform a conceptual design for the Orbital Debris Defense System (ODDS). The conceptual design of The ODDS considered the following:

1. Develop systems to positively impact debris population in the following size range:

- a. Greater than 2m.
- b. 2m. to 10 cm.
- c. less than 10 cm.

2. Research shielding technology for use in high debris population environments.

3. Research Tracking and Detection methods to improve the definition and capability to deal with the space debris problem.

**A3. Executive Summary.** Space debris has become a significant problem for nations interested in continued exploration and development of the space environment. The Orbital Debris Defense System (ODDS) deals with the space debris problem on all levels.

The nature and history of space debris has been researched extensively to gain a better understanding of the problem and how previous efforts to deal with the problem were developed. Each segment of the debris environment, grouped by size, small (< 10 cm), medium (10cm to 2 m), and large (> 2m) pose a different problem, and require a different solution. The biggest source of new debris, is old debris breaking up into smaller pieces. The obvious solution is to remove the most debris from orbit and do not contribute any more debris to the problem.

In this design, each debris size was dealt with individually. To remove the most massive pieces of debris, a vehicle was designed to deorbit large satellites and spent upper stages. A second vehicle was designed to collect medium debris for removal from orbit. Shielding technology was investigated to deal with the small debris population and use with orbital debris collection vehicles.



## SECTION B: MEDIUM DEBRIS

### Section Design Philosophy

As part of the Orbital Debris Defense System, the Medium Debris Collection Group was assigned to address debris in the size range from 0.1 meters to 2.0 meters. Research revealed that there were approximately 7000 pieces of debris within this range<sup>B1</sup> and that these pieces of debris were concentrated mainly in orbits of 800 km, 1000 km, and 1500 km<sup>B2</sup> (Figure B.1).

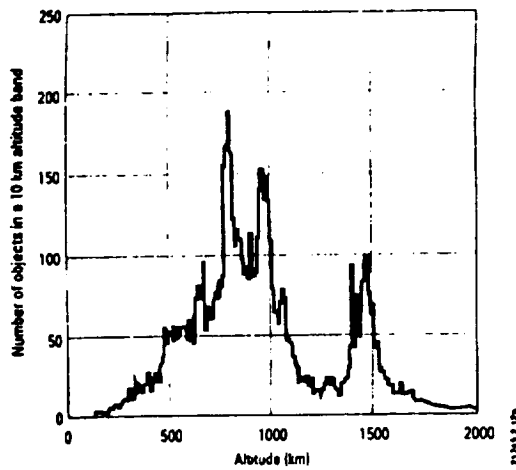


Figure 2-11. Altitude Distribution of Objects in Low Earth Orbit

**Figure B.1** Debris concentration at various altitudes.

The goal of the group was to collect as many pieces of debris as possible in the high concentration areas.

Current proposals to remedy the situation fell into one of two categories, active or passive collection. Active collectors seek out individual pieces of debris and are characterized by high fuel consumption. Passive collectors (or sweepers), on the other hand, are much larger satellites that

basically relied on flux models to collect debris. They are put into orbit with no specific path and collect debris by randomly colliding with it. The frequency of those random collisions is predicted through mathematical models called flux models<sup>B2</sup> (Figure B.2). The passive collector, therefore, is characterized by lower fuel consumption but lower collection rate, lower maneuverability, and much larger size.

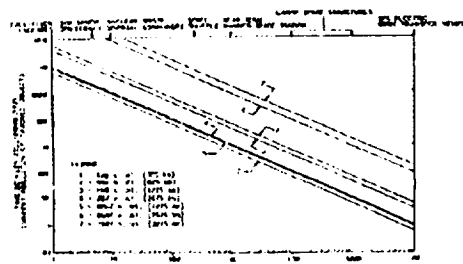


**Figure B.2** Debris flux graph.

The following sections contain a summary of various design configurations that were considered. A more in-depth discussion of the most promising of those designs follows.

### B1. Design Development

**B1.1 Passive Collection.** As a beginning, the Medium Debris Collection Group attempted to design a passive debris collector. The group decided to develop the idea of a butterfly net. The looseness (free-flowing) of the net would help to absorb an impact with debris. The net would have plenty of storage capacity and would need little maintenance. A conceptual drawing can be seen in Figure B1.1.1.

However, as Andrew Petro stated, 'In order to be effective, the sweepers would

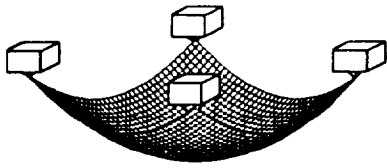


**Figure B1.1.1.** Schematic of debris particle with diameter  $d$  approaching a single sheet shield of thickness  $t_w$ .

have to be enormous, ...(with areas) of a square kilometer or more.<sup>B3</sup> To make an estimate of the weight of the net, it was assumed that the net could be modeled as a flat plate with a cross-sectional area of one square kilometer and a thickness one centimeter. Using a composite material, the weight of the net was found to be 13.9 million kg. In comparison, the weight of the space shuttle is 69,039 kg.<sup>B4</sup> Not only can the net not be launched using the shuttle engines, it could not be launched using the Titan IV-D, the launch vehicle chosen by the group. The Titan can launch 17,700 kg into low earth orbit.<sup>B5</sup>

The issue of avoiding working satellites, and therefore controllability of the net, became a problem. Further research also revealed problems with manufacturing a net of such size. It was found that a basal weaving system which uses a loom to form fabric in long, wide strips, would be most suited for this purpose. However, the net needed to be a kilometer wide and would therefore require stitching several strips together by hand. There would then be no guarantee that the net would hold.<sup>B6</sup> These problems, combined with the infrequency of

collection based on the flux model, forced the group to radically modify the design.

**B1.2 Quick Response System.** Identifying the collision or explosion of large debris as the main source of medium debris, a smaller, more mobile net was developed that would identify where a collision would occur or had just occurred and could be sent to sweep the area before the debris had a chance to spread out. As shown by Figure B1.2.1,<sup>B7</sup>, after an explosion, debris begins to encircle the earth.

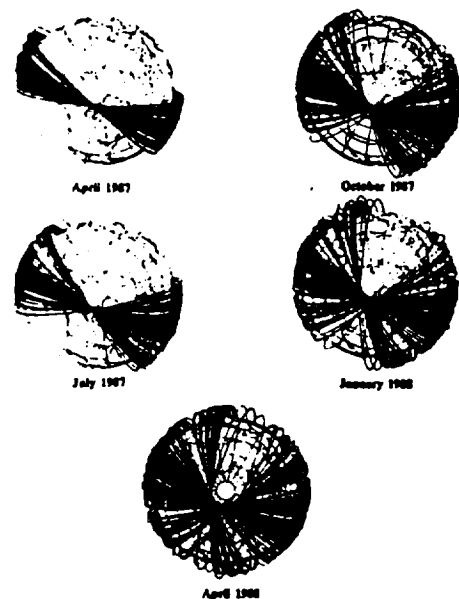


**Fig. 30** SPOT 1 R/S debris plume.

**Figure B1.2.1** Debris distribution of Ariane rocket explosion.

With a Quick Response System, the debris would be collected faster after a collision, thus keeping the debris area to a minimum.

This design forced the group to examine what the goal was. The group wanted to collect as many pieces of existing debris as possible. This design would wait for debris to be made before it would be sent to collect

it. Although this design may still work, it did not meet the design goal.

**B1.3 Impact Collector.** A device that would intercept debris and collect it using some type of shield, depending on the impact speed, was developed. For greater speeds, a shield that would vaporize the debris would be needed. For slower speeds, a shield in which the debris would become embedded would be required.

**B1.4 Cutter/ Grinder System.** Concurrently, an idea similar to the impact collector was being developed in the large debris collection group. These two ideas were so similar in objective and composition that they were integrated into a cutter/grinder device. Consolidated into a satellite shell, this device would rendezvous with a piece of debris by maneuvering from behind. Four conveyor belts would grab hold of the debris and bring it into the mouth of the satellite, where a pair of arc saws would sever the debris into many parts as seen in Figure B1.4.1.

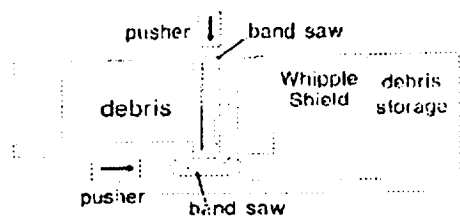


**Figure B1.4.1** Schematic of vehicle configuration.

One of the saws would cut a strip off of the piece of debris lengthwise and a pusher would then move this strip down. It would

then meet another arc saw which would cut the piece widthwise. The arc saws were chosen over conventional band saws due to the fact that band saws tend to break under heavy stress. The arc saw does not actually touch the debris and therefore does not produce stress on the blade. Likewise the arc saw would not produce a torque when cutting an object since the blade does not make contact with the debris piece and therefore increases the blade life. The cut pieces would then be moved by another pusher to a storage compartment located behind the saws.

The speed of the rendezvous would be kept to a minimum relative velocity (around 1-2 m/s) to ensure safety of the craft. The relative velocity would approach zero as the satellite overtook the debris to keep from using special handling of hyper-velocity and high-velocity impacts. A shield was to be placed in the rear of the satellite for the purpose of impacting with objects that were smaller than could be grabbed by the conveyor belts. The storage compartment could then be replaced when it reached maximum capacity. It would separate from the craft and would be replaced by an empty storage compartment on a refitting mission.

On the surface, this design appeared to be a worthwhile way to handle the medium debris problem. However, a closer inspection of the feasibility of this vehicle revealed that it was not a workable design. It was found that this device would consume vast amounts of power since most systems in the satellite were mechanically operated. The main power drain would come from the arc saws, since the cutting mechanisms were electric arcs. The power required for the saw alone would be in the area of 2.4 kW to 2400 kW, depending on the density of the material being cut.<sup>B8</sup> This power requirement was extremely high and did not

take into account the power required by navigation/communication system, the conveyor belts, or the pushers. Such a large power requirement could not be met with today's technology. The largest solar array ever used was on Sky Lab. It was designed to produce 20 kW theoretically, but in reality produced only 7 kW of useable bus power<sup>89</sup>. The solar array, if big enough, would be a good idea but the satellite would be moving in the dark side of the Earth and would be required to carry batteries to store power to be used while in the Earth's shadow. The battery requirement would make the weight of the satellite more than could be launched.

The four previous designs defined the following design criteria:

1. must be active collector
2. must fit weight and size restrictions of Titan IV-D launch vehicle
3. must use less than 7 kW of power
4. must collect existing debris

The final design that was developed met the all of the criteria above. It was an active collection unit. It fit both the weight (17,700 kg) and size (diameter < 5 meters, length < 19.8 meters) restrictions of the Titan IV-D launch vehicle. The power required to operate the system was less than 4 kW, and it addressed the current debris situation.

## **B2. Conceptual Design**

**B2.1 Mission Scenario.** Once in an 800 km elliptical orbit, from a successful launch on a Titan IV-D, the medium collector would be ready for its first capture. This altitude was picked due to the high concentration of debris in this orbit. The automatic systems would come on-line and

be ready for the initial commands for collecting debris sent from ground based tracking. After receiving a transmission on the location of the first targeted debris object, located in a 6° inclination from the satellite with a mass of 100 kg, the Medium Collector would fire the main thrusters to rendezvous with the first debris piece. In order to capture a debris piece, the Medium Collector would be required to approach the object from a lower orbit and from behind in order to reduce the relative velocity of the debris piece and the craft. After this maneuver the craft captured the object and used a total of 2876.53 kg of fuel.

The next debris location is received by the collector and the process begins again. Tracking orders the craft to change inclination by 3° to collect a 20 kg object. The thrusters fire to change inclination angles in order to capture the second piece. Again the craft moves in from below and behind and captures the debris piece using 1266.38 kg of fuel.

The craft awaits the next transmission from tracking which it receives shortly thereafter. The orders are to change inclination by another 3° to rendezvous with a 300 kg object. The craft slips into orbit with the debris object using 1160.62 kg of fuel to capture the piece of debris.

The Medium Collector is then ordered to perform an orbit change, using a Hohmann transfer, to an altitude of 1000 km over the surface of the Earth using 292.804 kg of fuel. From this position, the craft performs another inclination of 4° to collect a 150 kg object using 1411.606 kg of fuel in the process.

Upon completion of the previous maneuvers the Medium Collector prepares to move to an altitude of 400 km in order to be captured by the Space Shuttle. This maneuver insures that the remaining 3992.07

kg of fuel will be enough to allow the craft to return to the 400 km orbit with enough fuel to do small correction maneuvers while awaiting the rendezvous with the Shuttle. A listing of the computer program, written in Quick Basic is located in Appendix B1.

### B2.2 Layout.

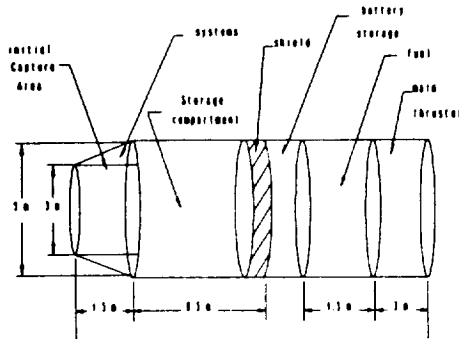


**Figure B2.2.1** Vehicle configuration

The group wanted to be able to make the vessel as large as possible so that maximum volume for fuel and collection purposes could be obtained. In order to determine the dimensions and weight of the collector vessel, it was necessary to determine the exact payload capacity for the Titan IV-D. The maximum dimensions for a payload in the Titan IV-D are a 5.09 meter diameter and a 19.8 meter length. The maximum weight the Titan can carry into Low Earth Orbit is 17,700 kg.<sup>B5</sup>

The group then set the dimensions of the vessel accordingly. The diameter was five meters with a three meter capture area. The length was set to 18.2 meters. This allowed the option of returning the satellite to Earth via Shuttle bay. Solar arrays cover 250 m<sup>2</sup> of the outside of the vessel. For safety purposes, the fuel and systems compartments were located in the outside meter of the cylinder as shown in the figure. This leaves a volume for the fuel and

systems of 228.7 m<sup>3</sup>.

**B2.3 Propulsion.** A Liquid Hydrogen / Liquid Oxygen propulsion system was used. The density of Liquid Hydrogen is 70.77 kg/m<sup>3</sup> when stored at -253°C. The density of Liquid Oxygen is 1138 kg/m<sup>3</sup> when stored at -183°C. The space shuttle uses a mixture which is 73% Hydrogen and 27% Oxygen by volume, and 86% Oxygen and 14% Hydrogen by mass.<sup>B4</sup> The Hydrogen / Oxygen mix has a specific impulse of 455 sec with an exhaust velocity of 4400 m/sec. The required volume was 37.5 m<sup>3</sup> for 13,731 kg of fuel. The volume left for the storage compartment was 128.6 m<sup>3</sup>.

The weight of the fuel was calculated by taking the maximum weight of the payload and subtracting off the structural and systems weights. The group began by assuming a weight of 150 kg for the avionics and navigation package. The solar arrays and batteries weigh 1833 kg. The outer cylinder is made of a protective composite shell with a thickness of 0.003 m and a density of 1386.9 kg/m<sup>3</sup>. The weight of the shell is 653 kg. The protection group estimated a shield weight of 1600. The propulsion mechanisms weigh an estimated 250 kg. Subtracting these weights from the maximum allowed for the Titan (17,700 kg), the fuel weight is 11000.

The number of maneuvers that can be made based on the calculated fuel weight depends on the method of collection. The collector can be set into one orbit and use fuel to change inclination angles, or it can be set to a given inclination angle and perform Hohmann transfers to change orbits. A combination of these maneuvers may also be used, depending on the specific mission. If fuel is used solely to change inclination angle, the collector will be able to maneuver 51° by 0.5° intervals, at an

altitude of 800 km. The total inclination angle will increase slightly with altitude, i.e. at 1500 km the total inclination is 53° by 0.5° intervals. The number of debris pieces that can be collected is based upon how much fuel it takes to collect each piece. A computer program (found in Appendix B1) was written that calculates the amount of fuel used in collecting a specific piece of debris and returns the fuel remaining for further collection. The program also takes into account the change in mass of the system as debris is collected and accordingly alters the velocity change required to propel the satellite. The satellite may need to slow down when impacting the debris, depending on debris size and shield design specifications, and then speed back up to maintain the current orbit. The program does not take into consideration any fuel that may be used for this type of maneuver because the rendezvous procedure has not been clearly defined. Figures B2.3.1 and B2.3.2 show plots of fuel consumption for inclination changes and Hohmann transfers, respectively.

**Fuel Use per inclination Angle**  
Liquid Hydrogen/Liquid Oxygen

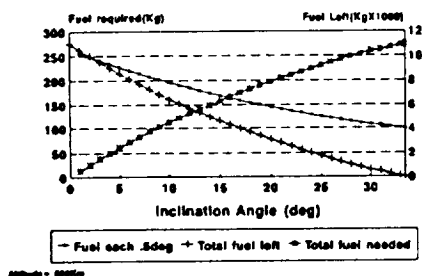


**Figure B2.3.1** Fuel use per inclination angle.

### Fuel Needed for Orbit Changes Hohmann Transfers from 800Km

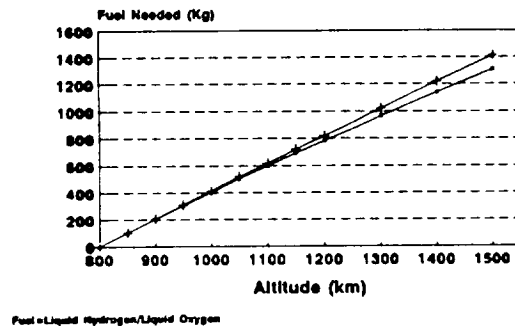


**Figure B2.3.2** Fuel needed for Orbit changes.

Appendix B2 contains several debris collection scenarios and the fuel used to collect each piece, as determined by the program.

**B2.4 Power Requirements.** The systems of the medium debris collection unit that required power were the propulsion unit, containment door, guidance, navigation and control unit, and the tracking unit. The GNC and tracking units required approximately a combined 2 kW of power. The containment door required an estimated 1 kW. The propulsion unit needed an estimated 1 kW for valve actuation. This brought the total required power to 4 kW. By covering the entire satellite with photovoltaic solar cells of specific power 6 W/kg and an efficiency of 14%,<sup>B8</sup> 25 kW of power can be generated. Assuming that only 30% of the satellite will be in direct sunlight, the average bus power output would be about 7.5 kW.

### B3. Conclusions

Orbital debris is a serious problem that threatens not only mission integrity, but human life. The Medium Debris Collection

Group was assigned to address the problem of debris in the range of 0.1 meters to 2.0 meters. The goal of the group was to collect as many pieces of debris as possible, thereby eliminating medium debris. Attempts to design both active and passive debris collectors were made. Passive collectors were found to be time inefficient. Problems with power requirements and fuel consumption were encountered with active collectors.

The group's final design minimizes power requirements by decreasing mechanical devices. The system was designed to provide the maximum amount of fuel possible. This was done by subtracting the weights of the necessary systems needed from the maximum launch weight of the Titan IV-D. The remaining launchable weight was left to be for fuel.

Problems with tracking and rendezvous may be encountered in later stages of the design. Stability problems may also arise as pieces of debris are collected and change the mass moments of inertia of the system. Further work needs to be done to describe better the debris situation.

The cost of the system also needs to be addressed. The group deems this as the ultimate deciding factor as to whether or not the system is built and used. Only when a better description of where individual pieces of debris are located can the exact number of debris that can be collected in one mission may be defined and the cost of collection per piece be found.

## SECTION C: LARGE DEBRIS

Erik Bedillion  
David Bragg  
Richard Demko  
Kelly James  
Tsuyoshi Kurosawa  
Enoch Ross  
Jeanette Simmons

### C1 Design Philosophy

**C1.1 Definition of Problem.** The targets of the large collection group are any and all objects with a dimension greater than two meters, particularly satellites which are no longer used, but still orbit the Earth in low orbits. Other objects, such as rocket bodies, large sections of fragmented satellites, and exotic items like the Hubble Space Telescope solar array, will also be targeted for collection. These objects, compose the most potentially devastating population of satellites orbiting the Earth. Any fragmentation of these objects, from explosive events or collision with smaller debris, will create a larger population of smaller debris which could start a domino effect that would eventually envelop the planet in a cloud of debris and limit the scope of the exploitation of near Earth space, also known as the "Kessler Effect."<sup>C1</sup>

**C1.2 Background.** Past and current proposals for the removal of debris from the near earth orbital environment have generally targeted small and medium debris. Methods include passive and active collection of these smaller objects and shielding to protect valuable satellites in orbit from collisions with the objects that cannot be collected. What has been proposed for larger objects, in this case satellites, includes passive drag devices, propulsive deorbit devices, and orbit escape

devices.

It has been suggested that all satellites that would be placed in orbits below 750 kilometers be equipped with a drag balloon which would reduce the orbit lifetime of a satellite by ninety percent when deployed. For objects orbiting above that altitude and below 25,000 kilometers, a propulsive deorbit device was suggested. These devices would also be placed on the geosynchronous orbit (GEO) transfer stages that would take satellites up to those higher orbits. At orbits greater than 25,000 kilometers, the most efficient and practical method for removing a satellite from the near Earth orbital environment would be the deployment of a propulsive or solar sail escape device which would drive satellite away from Earth into interplanetary space or towards the sun.<sup>C2</sup>

As described, however, these methods are for devices that will be integrated into satellite design and will be launched as a part of the satellite. There has been no serious attempt at designing or practicing methods to remove satellites already in orbit. Even though these methods would reduce the number of objects that would be left in orbit with future implementation, the problem of objects without such packages already in orbit still exists.

In March 1991, there were 1980 payloads in orbit.<sup>C3</sup> A large number of these objects have been in orbit since the 1960's, and many are objects that are no longer active and have been either left to decay naturally, a process of years or decades. Other satellites, such as those powered by nuclear cores, have been boosted to higher storage orbits. All of these objects, however, are still potential sources of smaller debris.



One method suggested for the removal of on-station satellites--those already in orbit without artificial means for deorbit--was the use of a modified orbital maneuvering vehicle (OMV). This OMV would be equipped for extended duration missions and a satellite retrieval package. Three modes of operation were identified for the OMV: direct deorbit; collection to a low-risk storage orbit; and attachment of a deorbit device, such as the propulsive or passive devices.<sup>C3</sup> However, the OMV is restricted to retrieving objects in orbits within a few degrees of the original inclination and no more than 1000 nautical miles above the initial orbit. Each retrieval would also be a single, dedicated mission, making this particular approach an economic impracticality.<sup>C4</sup>

**C1.3 Objective.** Because no feasible or practical approach has been defined for the removal of on-station satellites, the large collection group has undertaken the task of designing a system which would safely and reasonably dispose of such satellites, removing the largest potential source of orbital debris in the near Earth environment.

## **C2. Design Evolution and Development**

It was determined, despite the high cost of operation of the single-mission OMV, that one or more vehicles based on this concept would be the most effective method of removal of on-station satellites. Because the objects of concern are easily tracked from the ground with detailed orbital histories, complete rendezvous missions could be planned from the first orbital change of the vehicle to the interception of the target.

For practicality, the large collection group was split into two sub-categories of target size: satellites and debris. These two target

groups would require different methods for retrieval and disposal because of considerations of the immense differences in mass and dimensions of the targets and the composition of individual targets. Therefore, it was originally thought that two types of vehicles would be developed.

**C2.1 Debris Collection Unit.** Debris targets are mostly sections of rocket bodies and satellites that were produced from fragmentation of the primary body. This size range also includes such exotic debris as the solar array that was detached from the Hubble Space Telescope and released during the repair mission in December 1993. These targets are usually plate-like or small mass objects with at least one dimension greater than or equal to two meters.

The primary approach to development of a vehicle to intercept and collect these objects was an derivative of the vehicle designed to rendezvous with satellites, described later. Because these objects are of low mass and small dimensions, with respect to the larger, more massive satellites, it was determined to be impractical to attach a deorbit device to each item collected.

Two types of vehicles were developed. The first was a modular vehicle composed of a main propulsion unit, a storage unit, a processing unit, and the vehicle control unit. This vehicle could be deployed in various orbits. Because of fuel cost restraints for orbital altitude and inclination changes, it was envisioned that a constellation of a number of these vehicles would operate simultaneously in different "neighborhoods" of orbits. A "neighborhood" of orbits is composed of orbits within altitude and inclination ranges of 100 kilometers and 10 degrees with respect to

the vehicles current orbit.

Once in orbit, the vehicle would be assigned a target and would perform the appropriate orbital maneuvers to intercept the target. After the rendezvous is completed, the vehicle, approaching from behind the object to minimize relative velocities, would accelerate enough to overtake and swallow the object. Clamps would close down on the object to prevent movement while a conveyor belt inside would feed the debris through a series of cutting devices, similar to lumber being fed to a circular saw in a timber mill.

A number of cutting devices were considered. The first was using high-powered lasers, as is done in automated factories. Mirrors were considered to amplify the intensity of these lasers to cut up and vaporize the captured debris into manageable pieces. Lasers were rejected because of immense power requirements which could not be generated by any space-borne power source, such as solar arrays, batteries, or thermal nuclear generators. Saw blades, such as a band saw and a circular saw, were also considered, and tentatively accepted as the cutting devices for this vehicle.

After being fed through a primary blade which cut off a block of the object, a pusher moved the cut piece down into a chute oriented parallel to the entry chute. A second pusher fed the piece into a second blade and the smaller pieces were pushed into and stored in a module towards the aft of the vehicle, forward of the propulsion and the guidance, navigation and control (GNC) modules.

Once the storage module was filled or more fuel was required after numerous interceptions, a resupply vehicle launched on a smaller booster from Earth would

rendezvous with the collection vehicle. The main propulsion unit would separate and be refueled while the storage unit, now free, would also disengage itself from the vehicle. An empty storage unit would be attached in its place, the blades would be replaced if necessary, and the propulsion unit would be reattached. The collection vehicle would begin its new interception mission while the filled storage unit would fire small thrusters to enter a decaying orbit and burn up during atmospheric entry. This process would be completely automatic, with oversight from the ground. Refurbishment using the Space Shuttle was considered, but rejected for this and the other designs because of the high costs of such a mission and the enhanced dangers of astronauts working in such an environment. Destructive atmospheric entry was considered the best solution because there are dangers involved in the return of orbiting objects to Earth using the Space Shuttle.

The second design for the collection of debris was a complete unit similar to the first vehicle with only replaceable storage units, which were smaller than those of the modular vehicle and stored in cartridge unit. In design, it is similar to a semi-automatic pistol which is reloaded using a cartridge of bullets. Once a storage unit was filled, it would be ejected from the storage chamber and placed on a decaying orbit for destructive atmospheric entry. An empty unit would be moved from the cartridge unit into the storage chamber and connected and the collection vehicle could begin a new series of interceptions. Again, refurbishment of this vehicle was designed to be completely automatic, consisting of refueling the propulsion unit and replacing the storage unit cartridge.

After comparisons of work being done on

a design of a vehicle by the medium collection group, it was decided to merge portions of these two designs with the medium group's vehicle, primarily the cutting and storage units. The large collection group then focused its efforts on the vehicle that was being designed for the collection and disposal of satellites, the satellite collection unit.

**C2.2 Satellite Collection Unit.** The targets of this vehicle are all satellite payloads and the rocket bodies, such as upper stages and orbital transfer stages, that placed the payloads in their orbits. These targets are generally massive with large dimensions, ranging from a few meters and a few hundred kilograms to a dozen meters and several thousand kilograms.

Many satellites, especially communications satellites, are cylindrical for simple stabilization by spinning around the main inertial axis. Other satellites, such as reconnaissance and geodetic satellites, require more complex stabilization using thrusters or gravity-gradient methods because of the sensitivity of the cameras and other instrumentation carried on board. Still other bodies, especially the rocket bodies, are not stabilized. Some of these non-stable bodies tumble about the minor inertial axes resulting from some impact with another, smaller object.

All of these bodies and various states of stability were problems to consider when designing a vehicle that would rendezvous and dispose of deactivated satellites and spent rocket bodies. It was decided that the best method of disposal was to attach a deorbiting device of some type, such as the drag balloon or a propulsion unit.

Drag balloons were considered for a while,

for objects below 750 kilometers. However, there was the possibility of collision with other objects as the satellite was dragged down through the atmosphere. This was considered an uncontrollable situation with the potential for damage to or destruction of active payloads.

Because control of the deorbit process was preferred, a propulsive device was considered in the place of a passive system. A passive system was also believed to be more easily integrated into pre-operational design of the satellite. All satellites do not currently have deorbit packages designed into them, so the propulsive deorbit device must be attached to them in space.

The solution was using a clamping device at the end of the collection vehicle, also known as the Deorbit Modular Vehicle (DMV). This device was originally a pair of two flat plates of metal that were composed of smaller segments, allowing the plates to mold about a cylindrical object, such as a rocket body. Because of the dimensions of these objects, a jointed arm, similar to the robotic manipulator on the Space Shuttle, was added. The segmented plate was attached to a two-axis wrist, allowing for the collection of objects larger than the diameter of the collection vehicle. Once the target was secured in the clamps, the propulsive device would be attached to the outside wall.

To facilitate capture of these objects, a rotating ring was added to the collection vehicle. The robotic arms and clamp assembly were attached to the ring, which would rotate freely from the main body. During approach, the tumbling or spinning angular velocity of the target would be determined using an optical targeting system controlled by ground computers. After this

determination, the ring would be spun up using small motors and a gear assembly. Once the angular velocity of the ring equalled that of the object, relative velocity was eliminated and the object could be approached safely because the ring was mimicking the action of the target.

Final approach is made and the clamps are tightened about the object. Once secure, the ring motors would disengage and the ring would slowly despin the clamp assembly-target system. When angular velocity of the target and clamp reaches zero, the system is locked and attachment of the propulsive device could be facilitated.

Despinning of the satellite is necessary for two reasons. Attachment of the propulsive device would be complicated because a stationary object would have to be fastened to a rotating object. It is also possible that attachment of the propulsive device to the object would not necessarily be exactly on an inertial axis. If this were the case, firing of the rocket for re-entry could cause stability and control problems because of induced precession of the target about the spin axis. This precession would be amplified for as long as the rocket was fired, and would eventually cause a complete loss of control of the motion of the system. It is desired that control over the target during insertion into a destructive atmospheric entry orbit be complete. To ensure complete control over the system, it is necessary to remove the source of potential precession, the spin-stabilization of the satellite.

The propulsive device is simply a set of controllable thrusters, such as the hydrazine thrusters used for attitude control on normal satellites. These thrusters are controlled by a small GNC unit, which contains the fuel, and

are attached to the attachment unit. The entire unit is called the Deorbit Module (DOM).

Several methods of attachment were considered. The most common method was the use of a harpoon or a flachette, fired from the DOM into the relatively thin skin of the target. This was rejected because of the possibility of firing such a device into a component, such as a pressurized fuel tank or a still active electrical system, creating a potentially hazardous situation. Structural supports inside the target could also have prevented a secure attachment

The use of a magnetic device was rejected because most exterior shells of orbiting bodies are constructed of aluminum or aluminum alloys, non-ferrous materials with no magnetic characteristics. Adhesives were also considered, but rejected because of a lack of relatively flat surfaces on rocket bodies and satellites.

The final design of the DOM uses simple screws to attach the propulsion package securely to the target. The original concept of the screw was to take advantage of the angular momentum of a spinning satellite to provide the necessary torque for a screw to be secured to an exterior wall. However, there are many satellites which do not utilize spin-stabilization. Another problem arises if the screw is not attached to the device along the spin axis, causing an uncontrollable torque, so this approach was rejected.

Instead, a set of four screws would be utilized. The DOM attachment device would use four power drills, about the size of a modern cordless device, to drill four holes into the exterior wall of the target. Pre-drilled holes were considered necessary because of the large power requirements for driving a

screw directly into an unprepared metal shell. The DOM would then rotate inside the DMV so that the four attachment screws were lined up with the holes, creating a square. Power drivers would drive the screws into the holes and the DOM would be securely attached.

With this process complete, the DOM would be deployed from the DMV and allowed to fire its thrusters to enter a decaying orbit and burn up during atmospheric entry. The DMV would then continue on to its next target.

Several encounters by the DMV would consume its supply of DOV's and most of its maneuvering fuel. There are two options for the future disposition of the DMV. Automatic refurbishment is preferable because of the expense and danger of using astronauts and the Space Shuttle. New DOM's would be cartridge loaded into the DMV main body and the propulsion unit would be refueled.

The other solution is sending the DMV into a decaying orbit and burning up in the atmosphere. This should only be considered if the expense of constructing a new module is appreciably lower, in the long term, than the cost of periodic refurbishment of the DMV in orbit.

### C3. Deorbit Modular Vehicle (DMV)

#### C3.1 Mission Scenario

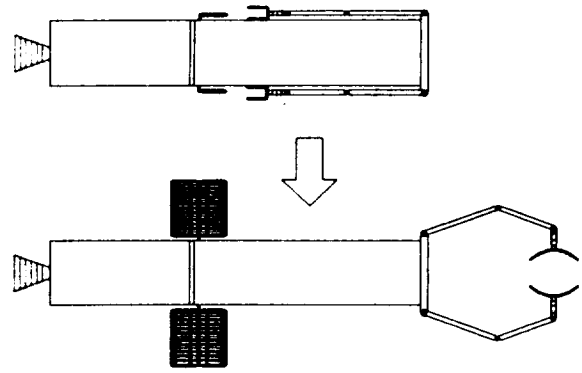


**Figure C3.1.1** The DMV converting from launch position to operational configuration.

After a clean launch atop a Titan IV Expendable Launch Vehicle from the Kennedy Space Flight Center, the Deorbit Modular Vehicle coasts towards its final orbit and the solar arrays extend to take in precious energy from the sun and storage batteries come on line to charge up while orbiting through the sun-side. Computers are activated and checks are run by self-diagnostics and ground controllers. Once testers are satisfied, the DMV brain goes on line to await its first mission.

Once batteries are fully charged after several revolutions, that mission is selected and assigned. An aging satellite in a highly elliptical, lower orbit is the target. If left alone, a freak collision with a tiny fleck of paint or a particle of solid rocket propellant might fragment that satellite into a cloud of dust and debris which would eventually envelop the planet and possibly start a chain reaction of collisions and fragmentations, spoiling near Earth orbit for proper exploitation. The computer brain of the DMV processes its mission. An exact plan for orbital transfer and rendezvous had been calculated by ground computers from the carefully tracked orbital elements of the target satellite.

A few last minute checks and the tiny maneuvering thrusters fire and the DMV orients itself and the main engine fires. A few moments pass, then the engine shuts down and the DMV begins its journey along the Hohmann ellipse which will bring it up behind and below its target somewhere on the other side of the planet.

An hour or so passes and the target is in sight of the DMV. The rendezvous is almost complete. The main engine roars to life for a second time and the DMV is inserted into an orbit just behind and below the target. While travelling thousands of kilometers per hour over the surface of Earth, the two objects, appear to hang quietly and motionless next to each other.

A pair of charge-coupled devices--special electronic cameras--turn on and several thousands of images are transmitted to a super computer on the ground. Seconds pass as several million computations are processed from the data presented by the images of the target. It is determined that the object is spinning about its primary inertial axis.

Another delay as the ground computer rapidly computes the required solution for the approach and capture. The DMV is to maneuver so that it is below and behind the target so that a small acceleration will bring it up perfectly centered about the axis of spin.

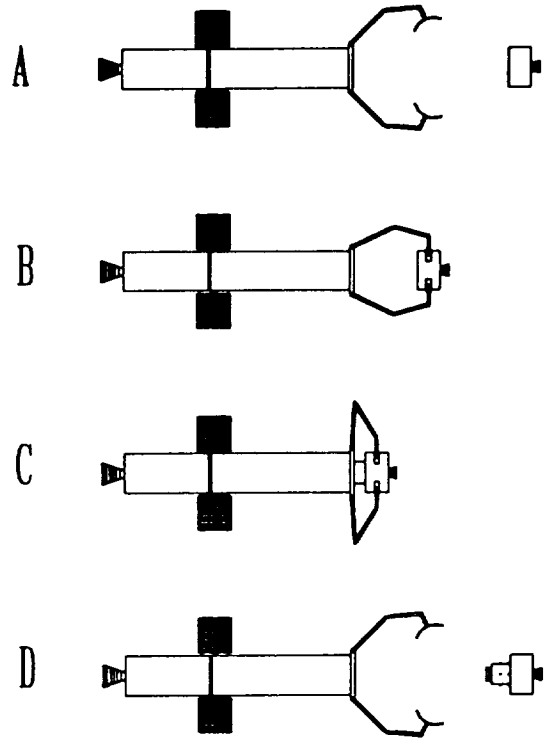


**Figure 3.3.1.1** Capture Scenario for DMV

Following the instructions from the ground, the DMV performs the required maneuver. Other instructions include the activation of the clamp assembly and the assembly spin ring. Two long, slender arms extend from their stowed positions outside of the mouth of the DMV. Two large, segmented plates fold up at the wrist of the arms and lock into position. Thirty minutes pass as the ring around the mouth of is spun up by small motors to match the angular velocity of the satellite about its axis. Finally, the system is ready (Figure C3.1.2A )

A tiny burst from maneuvering jets and the DMV accelerates forward towards the target. Seconds later, answering jets fire in the opposite direction and the DMV stabilizes. Positioning is perfect.

Arms unlock and move about to clamp the

target at a secondary inertial axis. Because the satellite is a cylinder, the plates swivel about their wrists so that they may mold themselves around the rounded shape, providing a solid grip. When a secure connection is made between the target's shell and the clamp, the arms lock and the target is now in union with the spinning clamp assembly (Figure C3.1.2B)

Batteries are connected to generators for charging from the power dissipated during the impending spin-down. Solar arrays are deployed for collection. Motors are idled and generators are connected. The ring responds to the reaction torque of the generators and begins to slow down from its spin, despinning the satellite with it. An hour passes and the satellite is no longer spinning. The system is now under control of the DMV.

The arms unlock again and maneuver the target for a solid connection with the mouth of the DMV, then lock again. Conveyor belts inside the DMV come to life and a Deorbiting Module (DOM) is moved forward until it is mated to the surface of the target (Figure C3.1.2C).

Inside the DOM, tiny drills come to life and drive forward into the outer skin of the target. After a suitable hole is drilled, the drills retract and the DOM is rotated so that screws line up with the holes. Tiny drivers then turn the screws, driving them into the holes and securing the DOM to the wall of the target.

Final checks are made. The ground computer completes its calculations and transmits its instructions to the DMV. When the DMV reaches the perigee of its orbit, thrusters are fired and the vehicle rotates so that it is now pointing back along the path of

the orbit and angled towards the surface. After a last minute check, the DOM is pushed out of the DMV by the moving conveyor belts, pushing the satellite forward with it (Figure C3.1.2D).

When a safe distance is reached, the DOM's complete array of engines fire at full throttle and a transfer begins. Within an hour, the DOM will have placed the satellite on a lower elliptical orbit that will drag it through the upper reaches of the atmosphere at its closest approach to the surface. Then, the pair will swing back to apogee at an altitude that almost reaches the perigee of the original orbit. Decay has begun and after a day or so, the new orbit will have circularized enough that drag will cause the satellite to plunge into the atmosphere and burn up. Its first mission complete, the DMV sits patiently in its orbit, charging up on precious power. When it is ready, its controllers will have another target for it to intercept and remove.

### C3.2 Structural Description

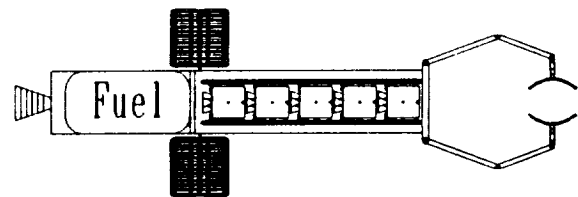


Figure C3.2.1 General layout of the DMV.

The complete layout of the DMV is presented in Figure C3.2.1. A pair of segmented plates are attached to a two-axis wrist at the end of a two-segment robotic arm,

similar to the robotic manipulator on the Space Shuttle. The plates are able to move in one longitudinal and rotate about that axis for different approaches and grasplings.

The arms are connected to a ring around the mouth of the DMV. Locks, similar to oarlocks on a rowboat, allow the arms to move along the body of the DMV, changing the grasping lengths of the whole assembly.

The ring is a large gear that is rotated by three motors to the required spin velocity for matching the angular velocity of the target satellite about its major inertial axis in the case of spin-stabilized satellites. If the object is tumbling about one of its minor inertial axes, the ring will spin around that axis to allow a secure attachment for stabilization. Two generators are also mated with the ring for power generation during the spin-down phase of operation.

The main body of the DMV is a simple shell containing five DOM's, the necessary control, guidance, power, and propulsion components and looks like a rocket body from the outside. Two large rectangular solar arrays are connect on folding wrists near the center, on a minor inertial axis for stability.

Inside, two conveyor belts with support shelves are located opposite each other and are embedded in the main walls of the DMV. These belts hold the DOM's during launch and move the DOM's forward to mate with the target satellite after it has been secured at the mouth of the DMV.

Aft of the DOM storage area is the guidance, navigation, and control module. Behind that is the power storage center, primarily composed of several arrays of battery cells. Liquid fuel and its oxidizer are

stored in the last third of the body, forward of the main engine. Hydrazine maneuvering thrusters are aligned along the minor inertial axes of the DMV.

**C3.3 Operational Components.** Because satellite technologies are well developed and proven in many types of applications, the large collection group chose to focus design work on the unique components of the DMV design, specifically the clamp and ring assembly and the DOM's. However, information concerning the requirements for operation of the DMV--such as propulsion, power, and control--are necessary for future design work.

**C3.3.1 Propulsion.** Main propulsion is provided by a bi-propellant thruster. The thruster selected is the TRW TR-201 thruster which has a specific impulse of 303 seconds and a thrust of approximately 44,000 Newtons. The fuel is nitrogen tetroxide and UDMH fuel.<sup>CS</sup> Approximately fifty percent of the total DMV mass is allocated for the propellant, storage tanks, and the main engine component. The main engine is the source of thrust for all orbital transfer maneuvers required for the interception of a target satellite. Because of high fuel costs, these transfers from the DMV's local orbit are limited to changes in altitude of about 100 kilometers and changes in inclination of approximately 10 degrees.

**C3.3.2 Power.** Electrical power will be supplied to all components, including the GNC, micro-hydraulic motors on the clamp, robotic arms, ring spin-up motors, and the DOM drills and screwdrivers. Power will be acquired using a pair of large, rectangular solar arrays. A bank of battery cells will store excess power derived from the solar



arrays for use during operation in the shadow of Earth.<sup>c6</sup>

Three types of solar cells were investigated to form arrays necessary to provide at least 1.5 kilowatts of power at a given time. These were silicon (Si), indium phosphide (InP), and gallium arsenide (GaAs). Silicon cells are the most common and oldest of solar cell technologies. The theoretical cell efficiency limit of these cells is in the range of 18 to 21 percent. They are also the most susceptible to degradation resulting from exposure to solar radiation in low Earth orbit. Silicon cells are, however, proven technology and they are the cheapest and lightest of the three types.<sup>c7</sup>

Gallium arsenide cells are a more recent solar cell technology. These cells are normally bonded to germanium bases for the generation of electrical power from solar radiation. The theoretical limit of their efficiency is approximately 23 to 25 percent, the highest of the three technologies. These are the densest of the cells. GaAs cells cost approximately \$155 per cell, compared to \$12 for the Si cells. Degradation of efficiency of the cells resulting from exposure to solar radiation is less than the Si cells, but higher than the InP cells.<sup>c7</sup>

A more recent innovation in solar cell technology is the indium phosphide cell. InP cells are almost as efficient as the GaAs cells, but are less dense and the least susceptible to degradation resulting from exposure to solar radiation in low Earth orbit. Their drawback is the highest cost because they are a newer development, about \$440 per cell.<sup>c7</sup>

After comparison of these characteristics, it was decided that the solar arrays would be made of the gallium arsenide cells on a germanium base. Though it was determined

in studies that a complete InP array required fewer cells to generate a kilowatt of power than the GaAs array, the cost proved to be prohibitive. The InP array had a relative cost per watt of 2 to 3 times that of the GaAs array. The silicon array, while half as much in relative cost, was almost twice the size of the GaAs array.<sup>c7</sup>

Performance, size, cost, and mass estimates for a 1.5 kilowatt array were determined from estimates provided for a 1 kilowatt array by multiplying the known estimates by 1.5, assuming linearity in these determinations. Thus, a 1.5 kilowatt array is composed of 12,575 cells and has an area of 11.175 square meters.<sup>c7</sup> Because of these sizes, it was decided to have two arrays with a power capacity of 1.5 kilowatts, producing a total of 3 kilowatts of power for use by all DMV and DOM systems. At the 1991 cost estimates for GaAs cells, cost of these arrays would be approximately \$3.89 million. However, these costs should decrease with time.

A rigid array is more efficient than a flexible array. However, it is necessary for the array to be stored in as small a space as possible for launching and for orbital transfers to prevent damage to the arrays. Therefore, the arrays will be a flexible array and will have a mass of 28.25 kilograms. Dimensions and mass include the support structure of the array. Array efficiency takes into account losses resulting from poor energy transfer and degradation effects.<sup>c7</sup>

Power will also be derived from generators connected to the clamp ring during the spin-down phase. It is estimated that there is a potential of several hundred watts of power generated during spin-down, depending upon the size and initial spin velocity of the target satellite. Excess power generated from these

operations will also be stored in the batteries.<sup>C6</sup>

The storage batteries will be nickel-cadmium cells. They are proven and the most extensively used of all batteries for spacecraft applications. It is desired to store 1.5 kilowatts of power in the battery array. Therefore, 22 cells are required and the total array will have a mass of 77.6 kilograms.<sup>C5</sup>

**C3.3.3 Guidance, Navigation, and Control.** Stability of the DMV will be maintained by a Mass Expulsion Reaction Control System (RCS). This type of attitude control system is typical for orbiting spacecraft and is used on such spacecraft as the Space Shuttle. It consists of three pairs of bi-propellant thrusters, each positioned on an inertial axis of the DMV. These thrusters allow for control in the three directions of motion: roll, pitch, and yaw. The roll and pitch thrusters are controlled by sensors which use Earth as an inertial reference. The yaw thrusters use connected to sensors which use sun or star position sensors for inertial guidance. These thrusters are the TRW MMPS thrusters and use monomethyl hydrazine (MMH) for fuel and each thruster has a specific impulse of approximately 305 seconds and a maximum thrust of approximately 400 Newtons.<sup>C5</sup> These thrusters will perform all minor attitude changes for repositioning of the DMV for interceptions and deployments of the DOM, as well as all attitude corrections and maintenance during the interception flight and the approach and capture procedures.

**C3.3.4 Tracking.** Tracking of target satellites for DMV operation will primarily be accomplished using the NORAD SPACECOM tracking network on Earth. Local targeting and tracking will be done using a pair of

charge coupled devices (CCD's) transmitting thousands of images for analysis and comparison by ground computers. These CCD's will allow ground computers to determine the relative angular and linear motion and momentum of the target satellite about any of its three inertial axes with respect to the body frame of the DMV in orbit.

**C3.3.5 Resupply.** If resupply of the DMV is deemed to be the most economical and practical option, it will be accomplished through automation. A fresh DOM cartridge and fuel will be launched to rendezvous with the DMV in orbit. After mating and fueling using procedures refined from in-flight refuelings by aircraft, the DMV will eject its empty DOM cartridge and mate with the fresh one. If the resupply vehicle is expendable, it and the spent DOM cartridge will be injected into a decaying orbit for destructive atmospheric entry. If it is a vehicle like the Space Shuttle or the Delta Clipper, it will return to Earth with the spent cartridge for refurbishment or recycling.

**C3.3.6 Orbital Deployment.** The DMV will be launched by the Titan IV ELV and boosted to its working altitude and inclination using its own propulsion unit. Because there are facilities at Kennedy Space Flight Center in Florida and Vandenberg Air Force Base in California, DMV's may be deployed to both polar and equatorial orbits, covering the full range of orbits that are used by American spacecraft from geosynchronous to retrograde polar orbits with inclinations of over 110 degrees. The Titan IV was selected because it is the largest American booster available.<sup>C8</sup> It is a derivative of a proven launch system and can launch into orbit a large range of payload sizes and masses. To get the largest number of DOM packages in orbit, the DMV

was assumed to be carried by the largest available payload faring for the Titan IV, approximately 26.2 meters long. This allows the DMV to be approximately 4.4 meters in diameter and up to 26 meters long. The maximum allowable mass for the DMV is 17,727 kilograms (39,000 lbs), the maximum mass that the Titan IV is able to place into a low initial circular working orbit of about 800 kilometers. Cost to launch the DMV on the Titan IV, in 1990 dollars, is approximately \$8,400 per kilogram. Total launch cost would be \$150.4 million in 1990 dollars.<sup>69</sup>

**C3.4 Capture Assembly.** The capture assembly consists of three major components: the spin ring, the robotic arms, and the plated clamp. This capture assembly, using simple technology and proven concepts, will allow the easy capture of most satellites and rocket bodies in orbit, even spinning or tumbling objects. Once capture is affected and stabilized, the deorbit modules may be attached and the target satellite is released and inserted into a decaying orbit.

**C3.4.1 Spin Ring.** The spin ring was designed to allow capture of objects that would be spinning--or tumbling--about one inertial axis. This ring, shown in Figure C3.4.1.1, is designed for use with a gear-reduction system and three drive motors. It is located at the mouth of the DMV and will spin independently of the main body during the capture process.

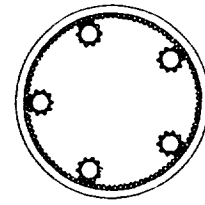


**Figure C3.4.1.1: Cross-sectional View of DMV Spin Ring with Spin Motors and Gear-Reduction Generators**

Prior to capture, the robotic arm/clamp assembly will fold up and lock into place from their stowed position along the body of the DMV. Using power stored in batteries in the aft portion of the main body, the three motors will spin the ring and clamp assembly to the designated angular velocity of the targeted debris. A concern during spin-up of the clamp assembly is the torques generated and their effect on the stability of the DMV. To obtain low torques during spin-up, a small angular acceleration is necessary and can be achieved with an extended time interval during spin-up. A  $\Delta t$  of 30 minutes will be implemented for spin-up operations. The majority of the targeted debris for capture will have spin stability angular velocities of less than 50 revolutions per minute. The torques generated versus angular acceleration for spin-up operations of the clamp assembly can be seen in appendix C.

During spin-up operations, attitude thrusters will fire to maintain the stability of the whole system, as is done for the Space Shuttle during satellite deployments and captures.

Power requirements for the original spin-up of the clamp assembly will be generated from the onboard batteries. Power requirements for spin-up of the clamp assembly to the required angular velocity of targeted debris can be seen in appendix C.

Once clamp assembly is at the required angular velocity, the DMV will be moved into position directly on the inertial axis about which the target is moving. With the arm-and-clamp assembly securely attached to the target, the motors are idled and the gear-reduction generators begin to despin the debris and clamp assembly.

These generators are connected to the main array of battery cells. Because the satellite has been in motion prior to this point, there will be a transfer of angular momentum from the system which now includes the ring and clamps to the gear-reduction generators. While a large portion of the energy from this transfer will be lost to friction, there is still a sizeable amount of useable energy. This is the energy that will be transferred through the generators to the storage batteries for later use by the DMV.

The added mass of debris upon capture by the clamp assembly causes additional torque problems as the despining of the clamp assembly and debris system takes place. A larger  $\Delta t$ , of about 60 minutes, will be needed for spin-down of the entire system to provide torques permitable for stability of the DMV. The power generated from the despining of the clamp and debris assembly that will be transferred to the generators onboard, versus the mass of the captured debris can be seen in appendix C. In order to assure burnup during re-entry, the targeted debris for capture will have masses less than 2500 kilograms. As with the spin-up operations, attitude thrusters will be used to keep the DMV stable during the spin-down cycle. Power for additional spin-up cycles will be drawn from the energy transfer to the generators. Also this power generated from the spin-down cycle will be implemented in the attachment of the DOM.

**C3.4.2 Robotic Arm.** The robotic arms that are the working arms of the clamp assembly are based on the manipulator arm on the Space Shuttle.<sup>C10</sup> The shoulder of each arm is a two-axis joint connected directly to the spin ring at the mouth of the DMV. The elbow is a single-axis joint and the wrist of the assembly is a three-axis joint, allowing for motion in all directions, including rotation of the clamp assembly for different grasping orientations during capture.

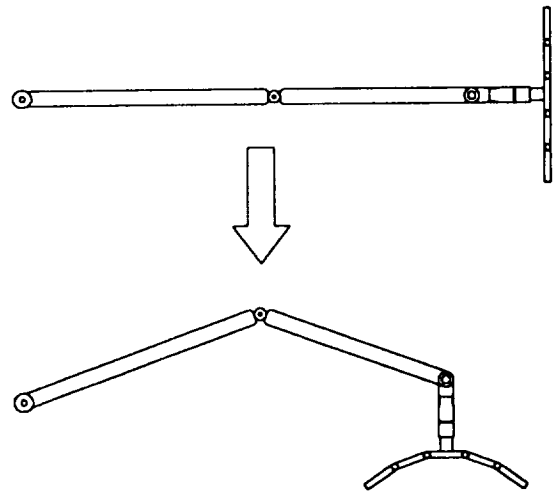


**Figure C.3.4.2.2:** Diagram of one robotic arm of the capture assembly, with the wrist and clamp attached to the end.

Each arm, as shown in Figure C3.4.2.1, is a thin-walled cylinder made of graphite-epoxy composite with insulating blankets protecting the composite from direct exposure to the harsh orbital environment. Total length of each arm is eight meters, fully extended, allowing a safe zone between the target and the DMV during the actual capture of the target.

The wrist, shown in Figure C3.4.2.2, will be designed to be as light, but as flexible and strong, as possible. Such weight reductions allow for a higher maximum load on the wrist and reduces the moment of inertia of the load

on the wrist.<sup>C11</sup>

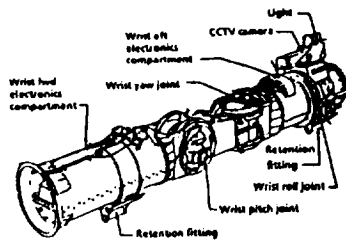


Figure 5-2.- Wrist joint.

Figure C3.4.2.2: Wrist of NASA Space Shuttle Robotic Manipulator Arm<sup>C11</sup>

This joint, and the shoulder and elbow, will have mechanical brakes attached to prohibit joint motion during critical moments, especially during spin-up and spin-down and the attachment of the DOM to the target satellite. This brake allows the arm to be manipulated and locked into place in different orientations. Locking of a particular joint also eases the positioning of another joint on the arm, as in the case of positioning the clamp on the surfaces of the target satellite during capture.<sup>C11</sup>

**C3.4.3 End Effector.** The manipulation of the end effector--a segmented plate--can be compared to a human hand with the fingers closed together and grasping a cylindrical object. It is composed of several independent plates of metal, positioned and manipulated like the individual bones of the fingers. The "knuckles" are micro-hydraulic joints which move the individual plates with one-degree of freedom.

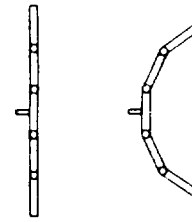


Figure C3.4.3.1: Front and Side Views of End Effector Composed of Five Segmented Plates

The end effector will be able to grasp objects with a minimum diameter of two meters and a maximum diameter of five meters. It will be able to effectively cover a surface area that is approximately eleven to twelve percent of the total surface area of the largest object and up to fifty percent of the surface area of the smallest object.

The basis for determining the number of plate segments and their dimensions was the mathematical expression of a circle with radius,  $r$ , inscribed in a polygon of  $n$  number of sides. The number of segments was determined by the percentage of the surface area of the object that was to be grasped. Various possible lengths for the segments, with varying debris sizes, were analyzed to determine the number of segments. It was concluded that five segments of dimensions 50 centimeters by 50 centimeters would cover the approximate surface area of an object needed to securely grasp it. The following mathematical expression for a circle inscribed in a polygon was used to determine the number of segments and their lengths:

$$\tan(\beta) = \frac{d}{l} \quad (C1)$$

$$\beta = \frac{\pi}{2} - \frac{\pi}{n} \quad (C2)$$

^A^P^A

^H^Ed. To resist erosion resulting from the friction that could be generated during the securing of the end effectors to the target, Molybdenum Steel was selected. This alloy of steel has excellent erosion resistance characteristics and is lighter and stronger than many other alloys of steel.<sup>B12</sup>

The aluminum alloy has a density of 2718 kilograms per cubic meter.<sup>B13</sup> Molybdenum steel has a density of 10220 kilograms per cubic meter.<sup>B12</sup> The mass of each segment of the clamping plate is 9.704 kilograms. Total mass of each complete clamping plate, without the hydraulic motivators, is 48.5 kilograms.

It is possible that the capture assembly might be spinning either faster or slower than the target. Therefore, to gain control of the spinning target, if this should happen, it is necessary to know the normal clamping force required to reduce the relative angular velocity between the end effector plates and the object to zero in a short period of time.

It was assumed that there could be as much as a five percent error in relative angular velocity of the spinning object to the capture assembly. The angular velocity of the target is a known quantity determined using the DMV's optical tracking system. Assuming a worst case scenario of a point mass located at the interface between the clamp and the target, the tangential acceleration of that point on the target's surface may be determined from the angular velocity of the target using the following expression:

$$a = \omega^2 r \quad (C3)$$

where  $r$  is the radius of the target and  $\omega$  is the relative angular velocity, assumed to be a maximum of  $\pm 2.5$  revolutions per minute, or  $\pm 0.262$  radians per second. The radius was assumed to be that of the maximum sized target, or approximately 3 meters. Therefore, the maximum tangential acceleration was calculated to be  $0.206 \text{ m/s}^2$ .

The interface was modeled as a simple point mass block on a relatively flat surface. A force acts upon the point mass because of the tangential acceleration. The mass was assumed to be half of the most massive object targeted, or approximately 1000 kilograms. Force equals the mass times the applied acceleration, or 206 Newtons.

To obtain the necessary static equilibrium between the clamp and the mass, there must be a friction force applied to the mass in the opposite direction of the force resulting from the applied tangential acceleration. Frictional force is directly proportional to an applied normal force on the mass. In this case, the normal force is that of the end effector plates being applied to the target. The required normal clamping force may be determined using the following equation:

$$N = \frac{F_f}{\mu} \quad (C4)$$

where  $F_f$  is the friction force equal to the tangential force and  $\mu$  is the coefficient of friction. The coefficient of friction was determined to be approximately 0.4 for Molybdenum Steel on Aluminum. For an object with a diameter of 6 meters and a total mass of 2000 kilograms, the normal clamping force required to reduce the relative angular velocity between the target and the plates is 515 Newtons for each end effector. For an object with a diameter of 2 meters and a

minimum mass of 200 kilograms, the tangential acceleration is  $0.068 \text{ m/s}^2$  and the required normal clamping force 17.16 Newtons. These numbers are well within the strength parameters of the steel and aluminum, which have yield strengths of 312 million Newtons per square meter<sup>B12</sup> and 275.65 million Newtons per square meter<sup>B13</sup>, respectively.

Each plate will have a micro-hydraulic device powering its motion, allowing individual manipulation. Hydraulic systems are used extensively in high-power robotic systems in the automated factories because of the large forces that may be applied for a relatively small package.<sup>C14</sup> These devices will be small by industry standards because the required force to hold the target satellite securely by the end effectors is of a magnitude of a few hundred newtons in a normal direction. Weight is not considered a load for the end effectors because of the micro-gravity environment, though mass is a large consideration when determining moments of inertia and controlling the motion of objects in orbit.

Each hydraulic device will be powered by a pump on the arm, which receives power from a storage battery that is charged during the spin-down process. The pumps must be on the arms or the spin ring because of the independence of the spin ring during the spinning cycles. To reduce hydraulic tube weights, the pumps will be placed as close to the effectors as possible and the tubes will be run inside the hydraulic arm to the wrist. Assuming a total equipment weight factor of approximately 1.5, the total mass of each end effector, including the hydraulic motivators, is 73 kilograms.

### C3.5 Deorbit Modules (DOM).

**C3.5.1 Attachment.** The attachment of the de-orbit module(DOM) is to be accomplished by screwing it onto the debris. In order to do this it is necessary to pre-drill the holes for the screws. This was accomplished by alternating a drilling unit and screwing unit around a circle (Figure C3.5.1.1). This allows the holes to be

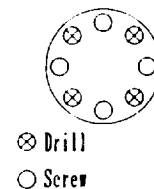


**Figure C3.5.1.1** Looking at base of module, the setup for the drilling and screwing units. drilled, and then by simply rotating the debris using the capture assembly, these holes will be lined up with the screwing units. The main draw back would be the power required to run the drilling and screwing units. In order to get an estimate on the power, additional analysis was performed.

The first thing that had to be determined was the length of each screw. The length screw was determined by examining the smallest size debris the DOM would have to go after. The debris was assumed to be a cylinder 2 meters in diameter with the module attaching to the side of it.. Using a CAD program, a scaled drawing of the debris and a 1 meter long line representing the base of the module were drawn. The CAD program was then used to find the distance between the base and the debris if the screwing units were placed in a circle with a diameter of 1 meter, shown in Figure C3.5.1.2.

A to B = .125m      Length:  
 B to C = .125m      A = .133975m  
 Diameter = 2m      B = .072975m  
 Length = 1m      C = .031754m



**Figure C3.5.1.2.** Sketch of system used to find length of screw.

The maximum distance turned out to be 13 centimeters. In order for the screw to be securely in place 5 cm of the screw should be in the debris. The design of the screwing unit (Figure C3.5.1.3) left about 2 cm of the screw

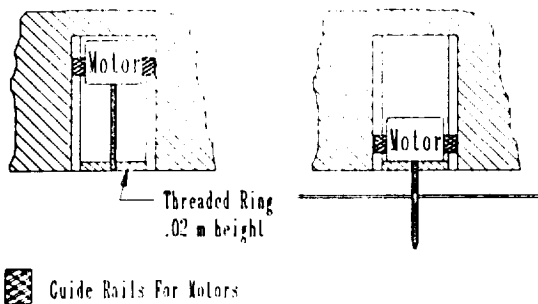


**Figure C3.5.1.3.** Diagram of screw unit before and after being insert into the debris.

inside the module. This made the total length of the screw to be roughly .2 meters.

The length was needed in order to determine the diameter of the screw needed to withstand the loads placed on it. The loading would come from the use of side thrusters to reorient the debris for the re-entry burn. The re-entry burn itself would be in line with the screws and place no significant load on them. Since the side thrusters had not been designed, a maximum side thrust of 450 newtons was chosen. This is representative of the thruster used on the Apollo Lunar Module. The Lunar module weighed over 14.5 metric tons fully

loaded, much more then any debris the DOM could handle<sup>C15</sup>.

To determine the diameter of the screw it was assumed that one screw would be taking all the load and there would be the maximum distance of .13 meters between the base of the DOM and the debris. The flexural stress on the screw was then examined assuming that the screw was securely placed in the debris and the skin of debris held. This allows the screw to be assumed to be a cantilever beam with a force P on the end of it. The force P is equal to the force of the side thruster. The stress formula used is the following:<sup>C16</sup>

$$\sigma_{\max} = \frac{M}{S} \quad (C5)$$

$$M = PL \quad (C6)$$

$$S = \frac{\pi d^2}{32} \quad (C7)$$

The symbol M is the moment due to the load, P, at the free end of cantilever and L is the length of the beam. A length of 13 cm and a load of 440 newtons were used to due a stress analysis on the screw with a diameter, d. An effective diameter,  $d_{\text{eff}}$ , is needed to model the crew as a circular beam. The effective diameter was derived using the standard formula used to find the stress area of a metric screw<sup>C17</sup>:

$$A = \frac{\pi}{4}(d-.9382p)^2 \quad (C8)$$

The term in the parenthesis can be assumed to be the effective diameter:



$$d_{eff} = d - .9382p \quad (C9)$$

Assumption that the skin of debris would hold when a force was applied to the hole made in it by the screw was made earlier. The feasibility of this assumption was analyzed by examining a 0.75 mm thick aluminum alloy 7075-T6 plate, with a 12 mm hole in it. The two cases of failure were examined assuming a force equal to P was applied to the inside of the hole. The first failure case involved the compression of the edge of hole. To examine this the following formula was used<sup>C16</sup>:

$$\sigma_b = \frac{P}{td} \quad (C10)$$

The resulting stress was 51.2 MPa, while the maximum yield stress for the aluminum alloy was 462 MPa. This gives a strength ratio, yield stress over the calculated stress, of 9.

For the second case a tensile failure of the sides of the hole was examined using the following formula<sup>C16</sup>:

$$\sigma_t = \frac{P}{2td} \quad (C11)$$

The tensile stress for the conditions stated before is 25.6 MPa. The maximum allowable stress is yield stress times 0.6<sup>C16</sup>, which is 277 MPa. This results in a strength ratio, maximum allowable stress over the calculated stress, of 10.8. So the assumption that the skin will hold the screw is feasible.

With the diameter of each screw known, the power required to pre-drill the holes could be estimated. The first step was to choose

some characteristics of the drill bit. The diameter should be roughly 3 mm smaller than the screw diameter to allow the threads of the screw to have material to bite into. This gave a drill bit diameter of 9 mm.

To calculate the torque and thrust required to drill into a material the drill bit design constants, A, B, and E needed to be chosen. These constants are based on the chisel edge width over the diameter of the drill bit, c/d, and if c/d is known a table in reference C18 can be used to find the constants. For a standard drill bit a c/d of 0.18 can be assumed for design purposes. This gives the following values: A=1.085, B=1.355 and E = 0.03<sup>C19</sup>.

The last three constants necessary to calculate the torque and the thrust are dependent on the material being drilled into (the working material). This preliminary design assumed that the structure of most of the debris will be aluminum. The working material constant, K, for aluminum it is equal 7,000<sup>C19</sup>. The cutting speed of the drill, CS, is 200 surface feet per minute for aluminum working material. English units were used because the equations for thrust and torque are based on english units, conversion factors will be applied to the final answer. The final constant that needed to be chosen was the feed rate of the drill, and it is based on a combination of working material and diameter of the drill bit. For aluminum and a diameter between 1/4 in and 1/2 in, the feed rate is 0.01 inches per revolution (ipr)<sup>C20</sup>.

With all the constants being known, the following equation can be used to calculate the torque and thrust required to drill the holes needed<sup>C19</sup>:

$$T = 2Kf^{0.8}d^{0.8}B + Kd^2E \quad (C12)$$

$$M = Kf^{0.8}d^{1.8}A \quad (C13)$$

where the torque,  $M$ , is in in-lbs and the thrust  $T$  is in lbs. For the diameter of 9 mm, and using the conversion factor 0.113, the required torque is 3.33 N-m. Using the conversion factor of 4.448, the required thrust is 325 N for a hole diameter of 9 mm.

The power (in kW) required to generate the torque,  $M$ , can be calculated using the following equation<sup>C19</sup>:

$$P_w = \frac{M \cdot N}{9550} \quad (C14)$$

$N$  is the rpm's of the drill bit and can be found using equation (17)<sup>C20</sup>:

$$N = \frac{3.82CS}{d} \quad (C15)$$

where  $d$  is the diameter of the drill in inches and  $CS$  is the cutting speed of the drill in surface feet per minute. The resulting power needed to generate a torque of 3.33 N-m is .754 kW for each drill.

To find the power required to generate the thrust needed, a type of drill press system must be chosen. For simplicity the system works on using two screws, on each side of the motor, which when turned will produce the thrust needed, as seen in Figure C3.5.1.4.

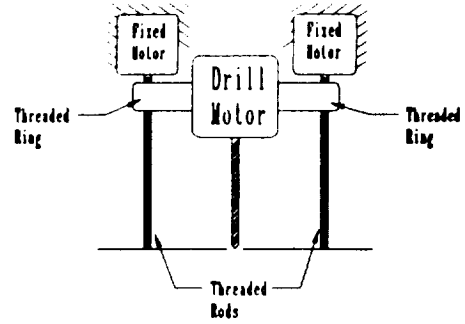


**Figure C3.5.1.4:** Drill Press for Deorbit Module Attachment

Equation 18 finds the require torque needed to produce a force  $F_t$ <sup>C16</sup>:

$$M = F_t r \tan(\phi_s - \theta) \quad (C16)$$

The force,  $F_t$ , is equal to half the thrust needed to drill (since there are two screws) and  $r$  is the radius of the screw, which was assumed to be 3 mm. The angles are defined as the following<sup>C16</sup>:

$$\theta = \arctan\left(\frac{L}{2\pi r}\right) \quad (C17)$$

$$\phi_s = \arctan(\mu_s) \quad (C18)$$

The distance between two threads is  $L$  and  $\mu_s$  is the coefficient of static friction. Coefficient was assumed to be 0.1. Finding the required speed for the screws to turn so they matched the require feed rate for the drill,  $f$  involved assuming a diameter for the screws and a  $L$  or pitch of the threads. A diameter of 12 mm and a pitch of 1.75 mm was assumed. Then using the following equation the rotational speed of screws in rpm was found.

$$SS = \frac{CSf}{L} \quad (C19)$$

The drill speed was calculated to be 313.1

rpm. Using equation (12) and (14) the power needed to produce the thrust 0.017 kW. The total power for the drilling unit is .771 kW.

The same equations can be used to get a general idea how much power is needed to drive in the screws. The force can be assumed to be roughly the weight of each screw, 0.8 N. The radius is equal to 6 mm and L is equal to 1.75 mm. Coefficient of static friction is assumed to be .1. The rpm of the screw is assumed to be 100 rpm. The necessary power is then .002 kW, but the screws will be self threading and will most likely require over 100 times the torque (roughly 500 N-m) to screw in, so the power will then be roughly 0.6 kW for each screwing unit. There needs to be at least two screws running in order make sure the DOM is attached level, so the about 1.2 kW will be needed for the screwing units at one time. Power required for the drilling and attachment of the screws to the target will be provided by the DMV.

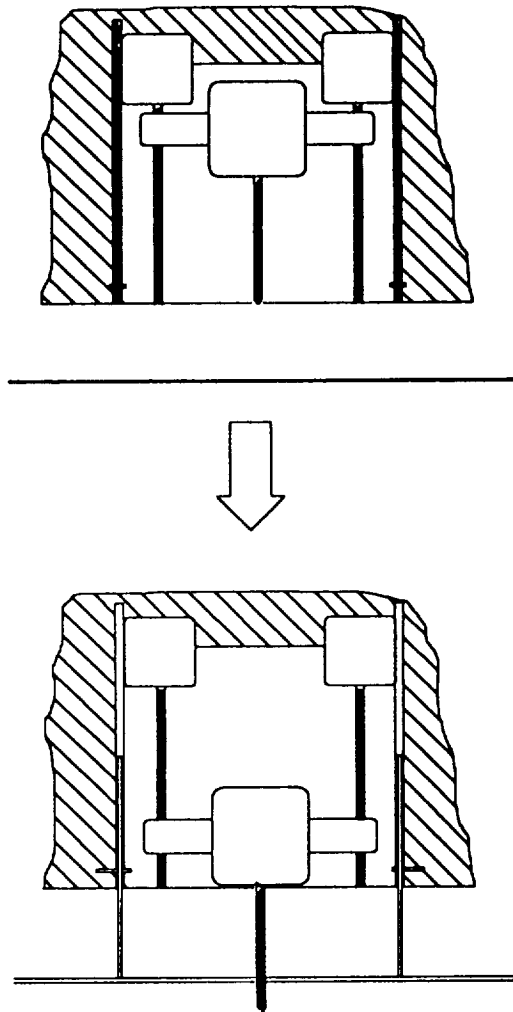


**Figure 3.5.1.5:** Schematic of Debris Containment Device for Use with DOM Drill Press

The problem of controlling the debris made by the drilling process was brought up. A possible solution to this problem is a tube device that would extend over the working area before drilling started and thus contain any debris made (Figure C3.5.1.5)

### C3.5.2 Propulsion

Transfers required to place the DOM and the target into a decaying orbit require a

orbital transfer. The simplest and most fuel efficient transfers is the Hohmann transfer because of the low orbital altitudes involved. This transfer is represented by two equations defining two impulses that change the velocity of the satellite. Because each orbit has a specific characteristic velocity, this change in velocity causes the satellite to change to the orbit which has the same characteristic as its new velocity. Normal operations require an initial impulse to enter an elliptical transfer orbit and a second impulse at the perigee of the transfer orbit to enter the new orbit. However, to reduce required fuel costs, only the first impulse burn will be performed to place the DOM and its target into an elliptical orbit that will slowly decay until destructive atmospheric entry:

$$\Delta v = \sqrt{\frac{2\mu}{a_1} - \frac{2\mu}{a_1+a_2}} - \sqrt{\frac{\mu}{a_1}} \quad (C20)$$

where  $\mu$  is the gravitational constant for Earth ( $39,860 \text{ km}^3/\text{s}^2$ ),  $a_1$  is the semi-major axis of the original orbit, and  $a_2$  is the semi-major axis of the target orbit, both measured in kilometers from the center of Earth.<sup>C21</sup>

The target altitude for the perigee of this orbit has been suggested to be 80 kilometers, inside the upper atmosphere.<sup>C2</sup> This altitude is low enough that atmospheric drag is significant enough to circularize the orbit and cause a rapid decay to atmospheric entry. Studies of required changes in velocity and the propellant necessary for the burn were done for an average spacecraft mass of 350 kilograms and an engine with a specific impulse of 310 seconds. For altitude ranges of circular orbits of 500 to 1500 kilometers, velocity changes to the 80 kilometer altitude ranged from 121 to 361 meters per second. Propellant mass required for these burns

ranges from 15 to 44 kilograms.<sup>C2</sup>

So that the DOM would be able to de-orbit satellites larger than 350 kilograms or located at the higher altitudes, it was decided to use a propellant mass of approximately 50 kilograms. The rocket motor selected was the Aerojet AJ110 bi-propellant hydrazine thruster, which has a specific impulse in vacuum of 320 seconds and a thrust force of 47,000 Newtons. The fuel it uses is UDMH and nitrogen tetroxide.<sup>C5</sup>

#### C4. Conclusion

All orbiting satellites, rocket bodies, and other large pieces of debris are potential sources of smaller, more numerous debris. Any collision could either simply knock off paint chips from or completely fragment these objects. It is vital to remove these objects from orbit once their mission life has concluded or they become uncontrollable or otherwise useless. If the major source is removed, the supply will slowly dwindle away to nothing naturally.

The DMV is an excellent option for the removal of large and massive objects that are currently in orbit because most of these objects have orbital lifetimes of centuries. The longer an object remains in orbit, the greater the possibility of collision and fragmentation as time passes. Controlled destructive atmospheric entry is one solution that ensures that objects will be removed from a potentially dangerous situation, and reduce the potential of danger for the objects that remain in orbit.

Of the limitations of this design, the greatest one is cost. It was estimated in a study done by NASA that developmental costs

for the single-mission OMV proposal would be approximately \$21 million (1988 dollars). Operation of the OMV would cost \$3.1 to \$3.7 million. If the Space Shuttle were used to operate the OMV at high inclinations from Kennedy Space Flight Center, that number would balloon to \$20.7 million.<sup>C4</sup>

Another limitation is the large mass of fuel that would be required to perform the number of orbital transfers and attitude adjustments to ensure a controlled interception, capture, and atmospheric injection. This translates into another cost limitation, as would the operational costs of resupply missions in orbit.

Fuel costs create the need for a number of vehicles to operate in several orbital neighborhoods simultaneously. While the production of multiple vehicles decrease developmental and construction costs down with time, the operational costs of several vehicles increases for the short term.

The time factor for each interception and capture is also of concern. One such mission would take close to one day. While it is assumed that automation could cover most aspects of each mission, there still must be human control to prevent potential disasters that would exacerbate the situation that is to be resolved.

There are other options when considering measures for the active reduction of objects in orbit around Earth. Of these are the inclusion of passive or active deorbit or orbital escape systems into satellite and upper stage designs. Drag balloons would be very effective in decreasing the lifetime of short-life satellites in very low orbits.<sup>C3</sup>

For satellites and upper stages in higher orbits, propulsive packages that are part of the

design would immediately insert the objects into decaying orbits for destructive atmospheric entry once their missions have been completed or loss of control occurs.<sup>C3</sup>

Satellites in geosynchronous and higher orbits could use deployable solar sails and propulsive packages to push them out of earth orbit into interplanetary space or towards the sun for disposal.<sup>C3</sup>

## **SECTION D: SHIELDING**

**Christopher Brown  
Kerri Knotts  
Lori Minick  
David Podner  
Taylor Strack**

### **D1. Section Design Philosophy**

Space debris and meteoroids of various sizes and velocities impacting the ODDS could decrease or have devastating effects on its structural integrity. An effective shielding system design for the ODDS is important to assure this integrity. The concept behind a shielding system is to intercept potentially disastrous debris particles and break them up into a cloud of solid, molten or vaporized fragments.

In the past, shielding consisted of thick, one layered metal, on the outer surface of a space vehicle. This protected the satellite mainly from meteoroids. With the increase in orbital debris the need arose for better shielding. In the 1930's Fred Whipple proposed the use of a double layer shield which became known as the Whipple shield<sup>D1</sup>.

Research for new types of shielding has been advancing over the last decade due to the growing awareness of orbital debris. Variations of the Whipple shield have been made due to satellite specifications or weight requirements. One such variation is the mesh double bumper shield. This shield saves weight by adding mesh and fabric which in turn decreases the amount of metal required<sup>2</sup>.

The multi shock shield is another variation of the Whipple shield where

several smaller layers are used instead of one bumper therefor saving weight. The MSS and MDB are presently being researched. Equations have been developed allowing these shields to be modified for different satellite requirements<sup>3</sup>. These shields are possibilities for use on the space station. Composite materials have also been researched to determine feasibility<sup>4</sup>.

Shielding technology was applied to the Deorbit Modular Vehicle (DMV), and the Medium Collection Unit. Both vehicles were designed with external shielding for protection of vulnerable operating components. The Medium Collection Unit will also include an internal shield as its primary collection mechanism. With the difficulty assessing survivability from space debris and meteoroids due to the uncertainties of particle mass, size, velocity, and conditions of the debris environment, analysis was done with expected on-orbit impact conditions.

By modifying existing shielding technology and studying the collision phenomenon between space debris and satellites, the appropriate shielding systems was designed for use with the ODDS.

### **D2. Description of Shields**

**D2.1 Basic Shields.** From research at NASA Johnson Space Center (JSC) Hypervelocity Impact Test Facility (HIT-F), many advanced shielding concepts have been developed. Currently, there are four types of common shielding systems. The single plate shield, Whipple shield, Multi-shock (MS) Shield, and the mesh double-bumper (MDB). The single plate shield shown in figure D2.1.1 is generally not used due to mass constraints leading to economic infeasibility.

### Single Sheet Shield

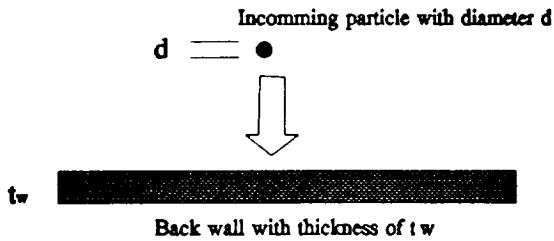


**Figure D2.1.1.** Schematic of debris particle with diameter  $d$  approaching a single sheet shield of thickness  $t_w$ .

D2

The Whipple Shield, figure D2.1.2, is the addition of a plate of material some distance from the structural shell of the spacecraft.<sup>D2</sup>

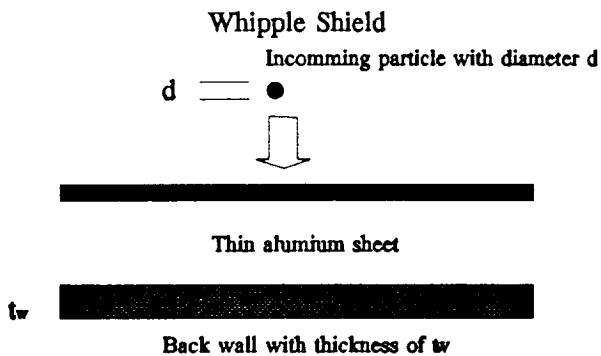


**Figure D2.1.2.** Schematic of a particle of diameter  $d$  approaching a cross section of a Whipple Shield with back wall thickness of  $t_w$ .

The idea is to break up the debris before it

gets to the structural shell. These basic concepts have led to some more advanced shielding technology.

**D2.2 Advanced Shields.** The Multi-shock (MS) Shield, figure D2.2.1, consists of four or five thin plates of material that repeatedly shock and vaporize the projectiles before they impact the rear wall (structural shell).<sup>D3</sup>

### Multi-Shock Shield

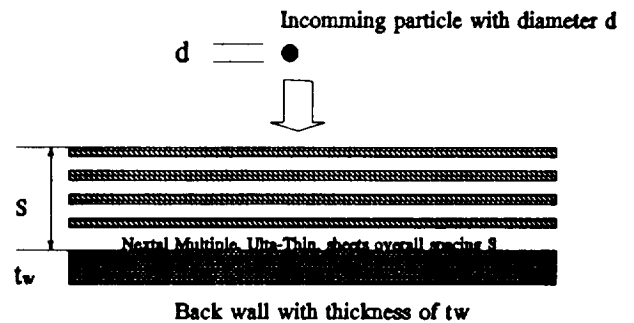


**Figure D2.2.1.** Schematic of a particle, diameter  $d$ , approaching a cross section of a Multi-shock Shield, overall spacing, and back wall thickness  $t_w$ .

The mesh double-bumper (MDB), figure D2.2.2, consists of four layers. A wire mesh to disrupt the projectile and spread the debris without substantially slowing the fragmenting particles, a second bumper to melt or vaporize the projectile fragments, an intermediate fabric to slow the debris cloud and any residual fragments, and a back wall to resist impulsive loading.<sup>D3</sup>

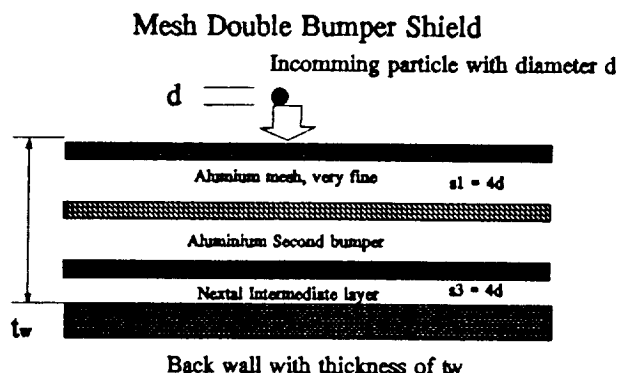


**Figure D2.2.2.** Schematic of a particle, diameter  $d$ , approaching a cross section of a Mesh Double Bumper shield, overall spacing  $S$  and thickness  $t_w$ .

In most cases, when the projectile penetrates an area of low mass (thin layers), high ejecta velocities can be expected; thereby, increasing the chances for vaporization. The MS Shield and MDB also provide tremendous weight savings compared to the single plate and Whipple shields.

### D3. Analysis of Shielding Technology

Considering the weight savings and the higher protection performance of multi-layered shields, equations for the MS and MDB shields presented by Christiansen (1993) were slightly modified and analyzed. Christiansen's equations solved for the diameter of the impacting projectile as a function of particle velocity, impact angle, overall spacing of the shield layers, and density of the particle. By rearranging these equations to solve for the back wall or

structural shell thickness, sizing of the shields needed was made possible. After inputting predicted particle diameters, the preliminary weight, shield thicknesses and maximum protection capability for the Medium Collection Unit and the DMV was established.

Particles impacting the Medium Collection Unit would be traveling at relatively low velocities due to the vehicle slowing in order to capture the debris. The MS Shield equations used in the calculations are relative for layers consisting of Nextel<sup>®</sup>, a ceramic fabric. The following equation determines the combined areal density,  $m_B$ , of all four Nextel<sup>®</sup> bumpers with an aluminum structural shell:

$$m_B = 0.19 d \rho_p \quad (D1)$$

where  $d$  is typically in the range of 10cm to 100cm.

The following equation for the thickness of the structural shell of each satellite is dependent on the velocity at which the particle is traveling, the impact angle, density, and diameter of the particle, the yield stress of the shield material, as well as, the areal density of the bumpers.

$$t_w = \frac{d \sqrt{\frac{\sigma}{40} (\cos\theta)^{\frac{3}{2}} \sqrt{\rho_p (V)}^{\frac{3}{2}}}}{2} - \frac{0.37 m_B}{\sqrt{\frac{\sigma}{40}}} \quad (D2)$$



where  $d$  is the diameter of the particle,  $s$  is the yield strength of the back wall,  $\theta$  is the impact angle,  $\rho_p$  is the particle density, and  $V$  is the particle velocity. Typical values for the previous parameters are the following:

$$\begin{aligned} d &= 0.1 - 1.0 \text{ cm} \\ \sigma &= 35 \text{ Kpsi} \\ \theta &= 0 - 60 \text{ degrees} \\ \rho_p &= 0.05 \\ V &= 1 \text{ km/s} \end{aligned}$$

Particles impacting the external portions of the DMV and the Medium Collection Unit will be traveling at an average velocity of 10 km/s<sup>D5</sup>. An alternative equation must be used to calculate the thickness of the structural shell according to Christiansen.<sup>D2</sup> The wall areal density is found using the following equation:

$$m_w = 41.7 M \frac{V_n}{S^2} \sqrt{\frac{40}{\sigma}} \quad (D3)$$

where  $M$  is the projectile mass. The wall thickness can now be found:

$$t_w = \frac{m_w}{\rho_w} \quad (D4)$$

The MDB Shield equations are relative for layers consisting of an Aluminum (alloy to be named) wire, an aluminum second bumper, a Nextel<sup>®</sup>, intermediate fabric, and Aluminum back wall. The mesh areal density is calculated by the following equation:

$$m_1 = c_m d \rho_p \quad (D5)$$

where  $c_m$  is an equation coefficient and  $d$  is typically in the range of 10cm to 100cm. The second bumper areal density can be calculated by the following equation:

$$m_2 = 0.093 d \rho_p \quad (D6)$$

The sum of the these two layers is represented by the following:

$$m_B = m_1 + m_2 \quad (D7)$$

The intermediate fabric layer areal density can be calculated by the following equation:

$$m_f = 0.095 d \rho_p \quad (D8)$$

The following equation for the thickness of the structural shell of each satellite is dependent on the velocity at which the particle is traveling, the impact angle, density, and diameter of the particle, the yield stress of the shield material, as well as the areal densities of the mesh, second, and intermediate layers. This equation is used for particles traveling at relatively low speeds.

$$t_s = \frac{d \sqrt{\frac{\sigma}{40} (\cos\theta)^{\frac{3}{2}} \sqrt{\rho_p} (V)^{\frac{3}{2}}}}{2.2} - \frac{0.37(m_B + m_f)}{\sqrt{\frac{\sigma}{40}}} \quad (D9)$$

Particles impacting the external portions of the DMV and the Medium Collection Unit will be traveling at an average velocity of 10 km/s. An alternative equation must be used to calculate the thickness of the structural shell.

$$t_w = \frac{m_w}{\rho_w} \quad (D10)$$

and  $m_w$  is found using the following equation:

$$m_w = 9M \frac{V_n}{S^2} \sqrt{\frac{40}{\sigma}} \quad (D11)$$

where  $M$  is the projectile mass. With the calculated thicknesses, the weight of can be determined for each shield.

## D4. Results

### D4.1 Mesh Double Bumper

The first set of results are for the Mesh Double Bumper shield.

Figure D4.1.1 is a graph of the internal shield thickness versus the particle diameter in groups of incidence angle. The graph is linear with a thicker shield generating a better protection. This was as expected.

### Mesh Double Bumper

#### Internal Shielding

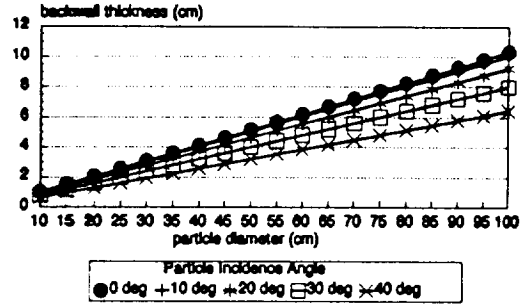


Figure D4.1.1 Internal shielding for Mesh Double Bumper; backwall thickness versus particle diameter at various particle incidence angles.

Figure D4.1.2 is a graph of the external shield thickness versus impinging particle diameter. Because the outside shield will be hit by particles of unknown incidence angle, an angle of 45° was assumed because this angle occurs most often. Again the graph was linear, and again this was as expected.

### Mesh Double Bumper

#### External Shielding

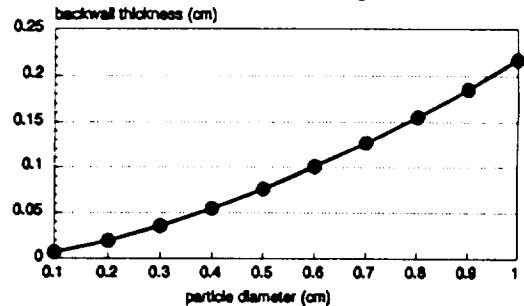
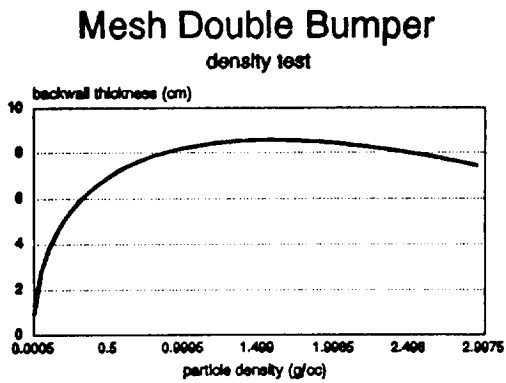


Figure D4.1.2 External Shielding Mesh Double Bumper; backwall thickness versus particle diameter at average incidence angle 45°.

Figure D4.1.3 is a graph of the thickness versus the particle density. This was done to check our estimation of .05g/cc as a

feasible density for the internal shield.



**Figure D4.1.3** Internal shielding Mesh Double Bumper; backwall thickness versus particle density for a 50cm particle at 45° incidence angle.

### D4.2 Multi-Shock

Figure D4.2.1 is a graph of the internal shield thickness versus the particle diameter in groups of incidence angles. The graph shows that the thickness is linearly proportional to the diameter and the incidence angle.

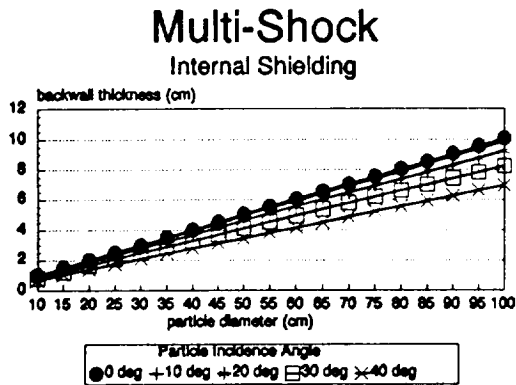


**Figure D4.2.1** Internal Shielding Multi-Shock; backwall thickness versus particle diameter for various incidence angles.

The Figure D4.2.2 graph is for the external shield. It shows the thickness of

the backwall versus the impinging particle diameter. To be used as a comparison to the mesh double bumper, an incidence angle of 45° was assumed. As for the interior case, the thickness is linearly proportional to the diameter.

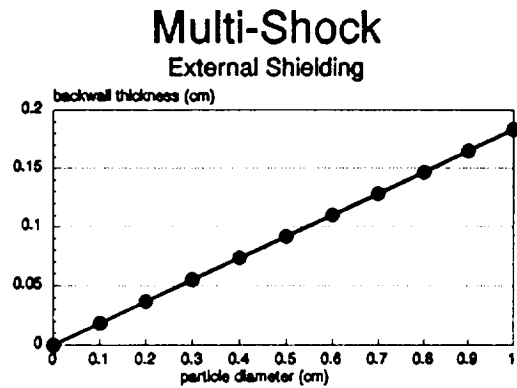


**Figure D4.2.2** External Shielding Multi-Shock; backwall thickness versus particle diameter for average incidence angle of 45°.

Figure D4.2.3 is a graph of the backwall thickness versus the impinging particle density. This was done to compare against the assumption of 0.05 g/cc for the density.

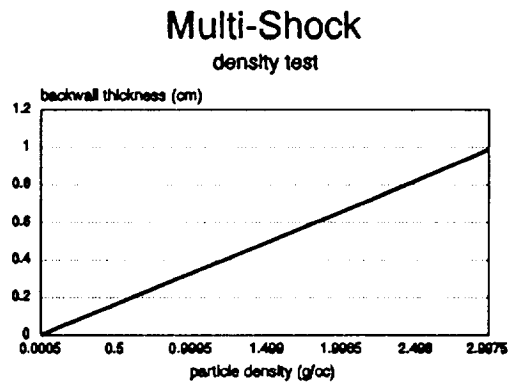


**Figure D4.2.3** Internal Shielding Multi-Shock; backwall thickness versus particle density for a 50 cm particle at a 45° incidence angle.

## D5. Conclusions

As can be seen from the graphs, as incidence angle is increased, the back wall thickness necessary to captivate an impinging particle decreases. Therefore, the shielding group decided to promote use of an angled shield. Due to the medium group's space limitations, the largest feasible incidence angle that can be used is 50 degrees.

The density test graphs (Figures D4.1.3 and D4.2.3) showed that the assumed value for density was acceptable in this case since it did not deviate from the expected curve.

The shielding group generated results for both the mesh double bumper and the multi-shock shield in order to more give more options to the medium group. The following conclusions are a result of Figure D4.1.1 (the mesh double bumper). Because the medium collection group wanted to protect against the largest possible projectile, a 4.66 cm back wall thickness was chosen. The final deciding factor in determining size was weight requirements. The medium group provided a maximum allowable shield mass of 2000 kg.

The mesh double bumper with the above specifications will require a mass of 1627.9 kg if the shield would be placed on angle of 50 degrees.

The multi-shock shield results were slightly different as can be seen from Figure D4.2.1. Again, in order to protect for the worst case scenario, a 6.7 cm back wall thickness was selected. However, this generated a mass of over 2000 kg for a 50 degree incidence angle.

Therefore, it is the shielding group's recommendation that for a 2000 kg mass restriction, the mesh double bumper shield will provide the most adequate protection.

The multi-shock shield would also capture the particles, but the added weight considerations make it a less feasible option.

## SECTION E: DETECTION/ TRACKING

By: Tom M. Rankin Jr.

### E1. Ground Based Tracking Systems

Detection and tracking, are necessary in locating debris in Earth orbit. Detection is different from tracking. Detection is the process of finding an object in Earth orbit and correlating the finding with that already logged in the satellite catalog. This is done by comparing the orbital elements of the object that has been "found" and those that have been deposited into the satellite catalog as a known object. Tracking and object is different in that the object is followed for a period of time in order to be further examined. Tracking debris in Earth orbit is necessary to ensure that manned space, flights as well as expensive equipment, are not damaged by even the smallest piece of debris.

According to the United States Space Command (USSPACECOM), there are approximately 7,000 tracked pieces of debris. USSPACECOM utilizes 26 different sensor systems to make up its space surveillance system which includes: phased-array radar systems, optical systems, and mechanical tracking radars. In deciding on the criteria for the ODDS craft, it was decided that the smallest piece of collectable debris be 10 cm. This was due to the fact that since most ground-based detection systems operate in the 500 MHz to 3 GHz range. At these frequencies particles 10 cm. and smaller appear as Rayleigh scatters.

It is expected that as larger debris is collected it will become easier to track smaller particles, which would require more computer time to effectively track. The time it takes to make a positive identification of a particle of debris is seen in Table 1 below.

Table E1.1. Track Length as Function of Object Period<sup>D1</sup>

OBJECT PERIOD LENGTH	TRACK (Minutes)
90	5
100	5.6
250	13.9
300	16.6
500	27.8
800	44.4

This is the time that it takes to correlate the orbital elements of a target piece of debris with the elements found in the satellite catalog. The capability of sensors to track is a fixed function of their total opportunities to track. It is also seen that it would be wise to attack the larger debris first because it is the cause of the smaller particles. If the satellite catalog were to double, the problem in tracking is resolved by upgrading equipment. If the catalog increases by a power of ten, then more computer, communication, and tracking systems will be needed. This makes it wise to collect larger debris first.

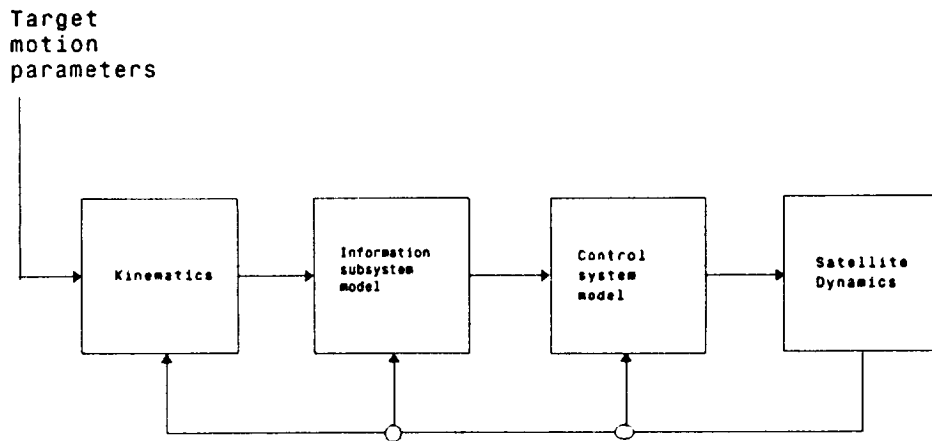
The ODDS vehicle (for both the large and the small/medium collectors) will be aligning itself with the particle of debris using the orbital elements of the debris that the ODDS is activated to retrieve. In order to make the ODDS vehicle easily tracked a beacon will be added. This will ensure that the ODDS craft will be easily located and no time will be spent on identifying the system. There will, however, be a large number of these crafts in orbit to make debris collection as swift as possible. This calls for a separate tracking system for the ODDS

system whose sole purpose is to follow the ODDS on its collection routes. This will mean an additional radar at the 26 different sensor stations. In adding this radar it then becomes necessary to follow the systems around the clock to ensure that the mission of each craft is being completed. This on a whole will save large amounts of computer time that is necessary for tracking smaller debris while ensuring the operational status of the system.

Other forms of homing devices that were examined were infrared systems similar to that on the IRAS system. This was not selected as a feasible system for on board of the ODDS craft due to its complexity. Lasers were also examined, but also were not acceptable due to weight and power requirements. For the debris problem, simple radar systems seemed to best for the small/medium debris collection group, and

Looking at the control of the ODDS craft, it is seen that it resembles a missile in its basic homing design. Below is a missile homing loop designed to fit the ODDS craft.

It is also correct to look at the control algorithm simplified to fit the model. The control algorithm provides continuous processing of data for the best final result in accordance with criteria on a priority scale and given limitations. For this particular system, only the simplest cases need examined. Some assumptions must be made to simplify the control of the crafts. First, the mathematical model can be simplified in the following areas: Kinematics, dynamics, and the control devises on the ODDS. Second, perturbations, noise, and operating conditions along with limitations on the homing system can also be simplified due to the space environment.



Missile homing loop made to fit a satellite model especially the ODDS craft

a radar/optical system for the large collection group, both of which are explained later.

## **E2. Large Debris Collection**

In collecting large debris for de-orbit it is necessary to be able to have depth perception for the clamp device. To achieve this it is acceptable to have an optical camera device that is linked directly to the ground.

When the ODDS craft that is responsible for large debris approaches its designated point in space with relation to the debris it is to attach to, control of the craft is turned over to human command. The cameras on the ODDS vehicle will send detailed observations to a computer on the ground that will control the attitude of the vehicle to match the motion of the satellite that is being retrieved exactly. There will be two cameras mounted on the craft so that a comparative analysis of the situation can be made. There will two cameras located on each of the flanges of the clamping device so that there is more control. Most, if not all; of this process will be performed by computers. A redundant system will be added to ensure that all problems that may occur are acceptably dealt with. There will also be the human control added to follow the mission and assume command if the need be. This will aid in the clamping procedure by ensuring that the clamp is in proper position to clamp, that the debris is not moving, and that the debris is indeed clamped into position for the drilling process.

## **E3. Medium Debris Collection**

The Medium Debris collection system is not quite as complicated as the Large Debris collection system. The initial stage of collection is the same as the large debris collector, in that ground-based radar systems

will guide the craft to the debris approaching from behind. The orbital elements will be matched except for the speed, which will be controlled in order to catch the debris slowly. Since the medium collector will be more of a "controlled crash", a space-borne radar is all that is necessary to actively track the debris upon closure to the debris. This is so that if the collector is hit by the debris in a way that will destroy the collector, the loss of the tracking system will be relatively inexpensive. The radar on the craft will take over when it has found the debris at a distance of 10 km. from the ground based radar systems. The on-board radar will make it possible for the collector to adjust speed and make minor direction changes to accommodate for the debris it is chasing. The debris will be tracked from the craft until it has been successfully "swallowed" by the craft. The vehicle will then be given new instructions for a different piece of debris.

## **E4. Conclusions**

In examining different tracking systems it is seen that it is effective to track from the ground and send the ODDS craft to the debris. If a passive system were to be used, there would be a number of years between captures, even if the ODDS craft were able to immediately respond to a partical of debris.

The tracking systems incorporated into the two different ODDS systems will be effective. The optical/radar system of the large debris collector will add depth perception, mimicking that of the Space Shuttles arm. There will be redundant systems that will operate in the case of an unforeseen accident.

The medium debris collector, even though

simple in design, is set up with a radar device that is effective and at a reasonable cost for this high risk satellite. The radar system also has a redundant unit in the event of a malfunction.

Many different types of systems were examined, and the most reasonable, yet cost effective systems were utilized for the project.

Et

ORIGINAL PAGE IS  
OF POOR QUALITY



## CONCLUSIONS

The Orbital Debris Defense System addresses the problem of orbital debris on several fronts. The recurring theme in all sections of the report is to remove as much debris as possible, thereby eliminating the major source for new debris. The different sizes of debris pose unique problems that require individual attention. Detection and tracking of debris is of absolute importance. It is impossible to collect or even simply to avoid what can not be seen. Knowledge of the size of the debris and its location is the first step in any solution.

The pieces of debris in the large range, due to their size, mass, and ability to be easily tracked are the most likely to be removed. The design of the DMV's Capture Assembly will allow it to target debris of widely varying size and orientations. The DOM's attachment scheme will allow it to be attached to almost any conceivable piece of debris within the size range. These factors plus the ability to be refueled and resupplied make the DMV a very solid solution to the problem of debris greater than 2 meters in size.

The amount of debris in the medium range, the area over which it is spread, and the distances between objects make it a particularly difficult problem. The size of the debris makes shielding of all satellites impractical, and the distribution makes collection difficult. The ability of the medium's group vehicle to easily collect any size debris makes it useful over a wide range of debris sizes. Its simple design should allow several vehicles to be in operation simultaneously.

The smallest range of debris, anything under 10 cm, is the largest segment of the debris population. The amount of particles, their distribution and size make it impossible to collect small debris, therefore satellites operating in space must be shielded. The shielding design philosophy, used here to design a shield for the medium collection vehicle, can be applied to other aspects of the orbital debris problem.

## RECOMMENDATIONS

The design presented in this report was a conceptual design and accomplished our goal of understanding the space debris problem and potential solutions. The fact that the design was a conceptual design means that many aspects of the mission scenario's and of the vehicles need further investigation before any solution can be recommended. Instead it is recommended that the proposed designs be investigated further into a preliminary design phase where feasibility and effectiveness could be assessed.

## References

- <sup>A1</sup> Kessler, Donald J. "Current Orbital Debris Environment," Orbtial Debris from Upper-Stage Breakup, *Progress in Astronautics and Aeronautics*, v 121, pp 3-13, American Institute of Aeronautics and Astronautics, Inc., Washington, D.C., 1989.
- <sup>A2</sup> Kessler, Donald J. "Current Orbital Debris Environment," Orbtial Debris from Upper-Stage Breakup, *Progress in Astronautics and Aeronautics*, v 121, pp 3-13, American Institute of Aeronautics and Astronautics, Inc., Washington, D.C., 1989.
- <sup>A3</sup> Kaczmar, Barbara Woods, "Junkyard in the Sky" *New Scientist*, v 128, pp36-40, October 13, 1990
- <sup>B1</sup>. Scott, W.B., "Russian Politics May Stymie Laser/Optics Collaboration," *Aviation Week and Space Technology*, March 21, 1994
- <sup>B2</sup>. Reynolds, R.C., Ruck, G.T., "Final Report on an Assessment of Potential Detectors to Monitor the Manmade Orbital Debris Environment," NASA, Johnson Space Center, NAS9-16721
- <sup>B3</sup>. Petro, A.J., "Techniques for Orbital Debris Control," *Journal of Spacecraft and Rockets*, Vol. 29, No. 2, March-April 1992
- <sup>B4</sup>. Shayler, D., *Shuttle Challenger*, Prentice Hall Press, New York, 1987
- <sup>B5</sup>. Apollo Spacecraft News Reference, Grumman Aircraft Engineering Corporation, Bethpage, NY 1969.
- <sup>B6</sup>. Bingul, F., "Textiles in Composites, A Literature Review," MAE Dept., WVU
- <sup>B7</sup>. "Cutting Techniques as Related to Decommissioning of Nuclear Facilities," Nuclear Energy Agency, February 1981
- <sup>B8</sup>. Woods-Kaczmar, Barbara, "Junkyard in the Sky",
- <sup>B9</sup>. McKay, M.F., McKay, D.S., Duke, M.B., "Space Resources, Energy, Power, and Transport," NASA, Johnson Space Center, 1992
- <sup>C1</sup>Kessler, Donald J. "Current Orbital Debris Environment," Orbtial Debris from Upper-Stage Breakup, *Progress in Astronautics and Aeronautics*, v 121, pp 3-13, American Institute of Aeronautics and Astronautics, Inc., Washington, D.C., 1989.
- <sup>C2</sup>Petro, Andrew J. and David L. Talent, "Removal of Orbital Debris," Orbtial Debris from Upper-Stage Breakup, *Progress in Astronautics and Aeronautics*, v 121, pp 169-182, American Institute of Aeronautics and Astronautics, Inc., Washington, D.C., 1989.
- <sup>C3</sup>Satellite Situation Report, v 31, n 1, National Aeronautics and Space Administration, Goddard Space Flight Center, Greenbelt, MD, 31 March 1991.
- <sup>C4</sup>Petro, Andrew and Howard Ashley, "Cost Estimates for Removal of Orbital Debris," Orbtial Debris from Upper-Stage Breakup, *Progress in Astronautics and*

*Aeronautics*, v 121, pp 183-186, American Institute of Aeronautics and Astronautics, Inc., Washington, D.C., 1989.

<sup>C5</sup>Perini, Richard J. and James L. Hanson, "Three-Axis Electrohydraulic Robotic Wrist," *SAE Technical Paper Series*, Milwaukee, WI, September 1989.

<sup>C6</sup>Bryan, Mark K., "Payload Deployment and Retrieval System, Nominal Operations," Lyndon B. Johnson Space Center, Houston, TX, December 1988.

<sup>C7</sup>*ASM Metals Reference Book*, 2nd ed., American Society of Metals, 1983.

<sup>C8</sup>Apollo Spacecraft News Reference, Grumman Aircraft Engineering Corporation, Bethpage, NY 1969.

<sup>C9</sup>Cheng, F., *Statics and Strength of Materials*, Macmillan, New York, 1985.

<sup>C10</sup>Wick, C. (ed), *Tool and Manufacturing Engineers Handbook*, Vol 4, pp. 8-11 to 8-12, Society of Manufacturing Engineers, New York, 1987.

<sup>C11</sup>*Annual Book of ASTM Standards*, Vol 15.08, F 468M-84b, pp 250-252, ASTM, Philadelphia, PA, 1990.

<sup>C12</sup>Wick, C. (ed), *Tool and Manufacturing Engineers Handbook*, Vol 1, pg. 9-79, Society of Manufacturing Engineers, New York, 1983.

<sup>C13</sup>Krar, S.F. and J. W. Oswald, *Drilling Technology*, pp 60-61, Delmar, Albany, NY, 1977.

<sup>D1</sup> Palais-Cour, Burton G. and Avans, Sherman L., "Shielding against debris," *Aerospace America*, June 1988, pp.24-25.

<sup>D2</sup> Christiansen, Eric L., and Kerr, Justin H., "Mesh Double-Bumper Shield: A Low-Weight Alternative for Spacecraft Meteoroid and Orbital Debris Protection," *Int. J. Impact Engng*, Vol. 14, 1993, pp. 169-180.

<sup>D3</sup> Christiansen, Eric L., "Design and Performance Equations for Advanced Meteoroid and Debris Shields," *Int. J. Impact Engng*, Vol. 14, 1993, pp. 145-156.

<sup>D4</sup> Chaturvedi, Shive K., and Sierakowski, Robert L., "Effects of Impactor Size on Impact Damage-Growth and Residual Properties in an SMC-R50 Composite," *Journal of Composite Materials*, Vol. 19, March 1985, pp. 100-113.

<sup>D5</sup> Cour-Palais, Burton G., "Hypervelocity Impact Investigations and Meteoroid Shielding Experience Related to Apollo and Skylab," pp. 247-260.

<sup>D6</sup> Christiansen, E. L., Robinson, J. H., Crews, J. L., Olsen, G. D., and Vilas, F., "Space Station *Freedom* Debris Protection Techniques", *Adv. Space Res.*, Vol. 13, No. 8, 1993, pp. (8)191-(8)200.

## Appendix B

```

CLS
DIM SHARED MP(8000)
Pi = 4 * ATN(1#)

INPUT "What is the initial mass of the spacecraft?(kg)"; MI
INPUT "What is the maximum mass of the fuel the S/C can hold(kg)?"; MF
INPUT "What is the specific impulse of the propellant(sec)"; Isp
INPUT "What is the escape velocity(m/sec)"; Ve
GOTO 5

1
5
CLS
INPUT "Type OB for an orbit change or IA for an inclination angle maneuver"; a
IF (ans$ = "OB") OR (ans$ = "ob") THEN
  GOTO 30
ELSEIF (ans$ = "IA") OR (ans$ = "ia") THEN
  GOTO 40
ELSE
  GOTO 5
END IF

40
INPUT "What increments of inclination angles for the orbit you desire(DEG)";
INPUT "How many degrees are you changing(DEG)"; DEG
INPUT "What is the orbit distance from the surface of the earth(Km)"; h
PRINT "What is the expected amount of mass to be collected in this"
INPUT "particular orbit.(Kg)"; DEB

Di = ABS(Di)
DEG = ABS(DEG)
g = Ve / Isp
nu = 398601!
r = (h + 6378.135)
Vc = (nu / r) ^ .5
Di = Di * (Pi / 180)
ang = SIN(Di / 2)
Dv = 2 * Vc * 1000 * ang
PRINT "Propellant(kg)      Angle of inclination"

U = 0
MUI = 0
FOR x = 0 TO DEG STEP Di
  MP(U) = MI * (1 - EXP(-Dv / (Isp * g)))
  x = x + Di * (180 / Pi)

  PRINT USING "####.####      ##.###"; MP(U); x

  MI = MI - MP(U)
  MUI = MUI + MP(U)

35
SLEEP
U = U + 1
NEXT x
MI = MI + DEB
MFF = MF - MUI
MF = MFF

```

```

PRINT "YOUR SPACECRAFT BURNED THE AMOUNT OF FUEL SHOWN BELOW:"
PRINT USING " #####.###^ ^ ^ (KG)"; MUI
SLEEP
GOTO 100

```

```

100
CLS
IF MF = 0 THEN
PRINT "THERE IS NO MORE FUEL LEFT IN THE SPACECRAFT!!!"
ELSEIF MF < 0 THEN
PRINT ""
PRINT ""
PRINT "YOUR LAST MISSION REQUIRED MORE FUEL OF WHAT WAS LEFT"
PRINT "YOU WILL HAVE TO REPEAT YOUR ENTIRE MISSION"
SLEEP
GOTO 60
ELSE
END IF

```

```

INPUT "Do you want to perform another maneuver(Y/N)"; typ$
CLS
IF (typ$ = "Y") OR (typ$ = "y") THEN

PRINT USING " You have #####.## kg of fuel left"; MF
SLEEP
GOTO 1
ELSEIF (typ$ = "N") OR (typ$ = "n") THEN
GOTO 60
ELSE
GOTO 100
END IF

```

```

30
INPUT "Distance from the surface of the earth for the first orbit(km)"; r1
INPUT "Distance from the surface of the earth to the second orbit(km)"; r2
PRINT "What is the expected amount of mass to be collected in this"
INPUT "particular orbit.(Kg)"; DEBS$

```

nu = 398601!

```

a1 = (6378.135 + r1)
a2 = (6378.135 + r2)
a = (a1 + a2) / 2

```

```

Dv1 = (((2 * nu) / a1) - ((2 * nu) / (a1 + a2))) ^ .5 - ((nu / a1)) ^ .5
Dv2 = ((nu / a2)) ^ .5 - (((2 * nu) / a2) - ((2 * nu) / (a1 + a2))) ^ .5
Dv = (Dv1 + Dv2) * 1000

```

```

10 MPP = MI * (1 - EXP(-Dv / (Ve)))
Dt = Pi * ((a ^ 3 / nu)) ^ .5
MP = ABS(MPP)

```

```

PRINT "PROPELLANT BURNED DURING THE MANEUVER (Kg). "
PRINT USING "#####.### "; MP

```

```
PRINT "Time spent(sec)"
PRINT USING "####.###"; Dt
MFF = MF - MP
```

21

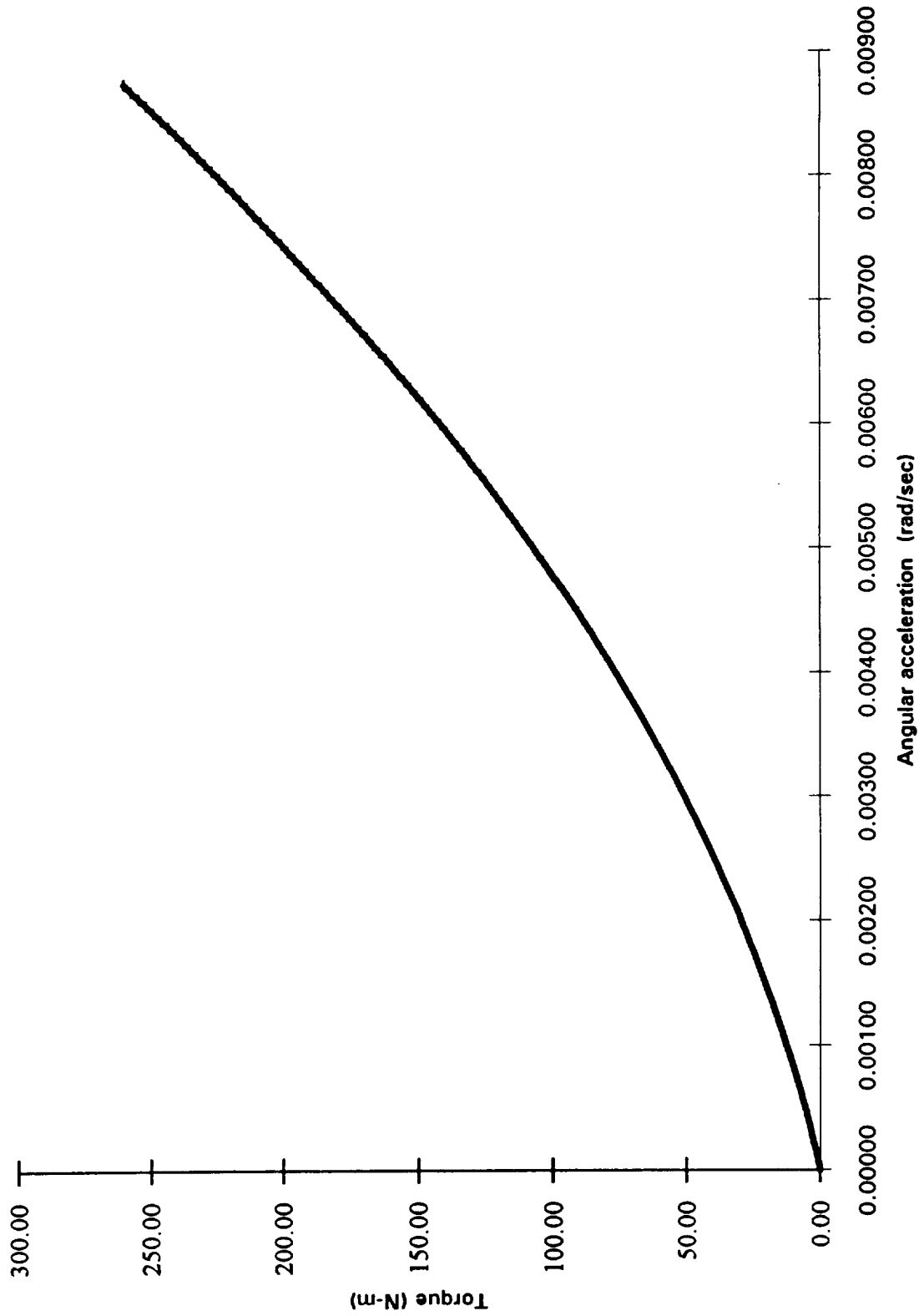
```
PRINT USING "You have #####.## Kg of fuel left."; MFF
MI = MI - MP + DEB
MF = MFF

IF MF = 0 THEN
PRINT "THERE IS NO MORE FUEL LEFT IN THE SPACECRAFT!!!"
ELSEIF MF < 0 THEN
PRINT ""
PRINT ""
PRINT "YOUR LAST MISSION REQUIRED MORE FUEL OF WHAT WAS LEFT"
PRINT "YOU WILL HAVE TO REPEAT YOUR ENTIRE MISSION"
SLEEP
GOTO 60
ELSE
END IF
```

```
INPUT "Do you want to perform another maneuver(Y/N)?"; orb$
IF (orb$ = "Y") OR (orb$ = "y") THEN
GOTO 1
ELSEIF (orb$ = "N") OR (orb$ = "n") THEN
GOTO 60
END IF
```

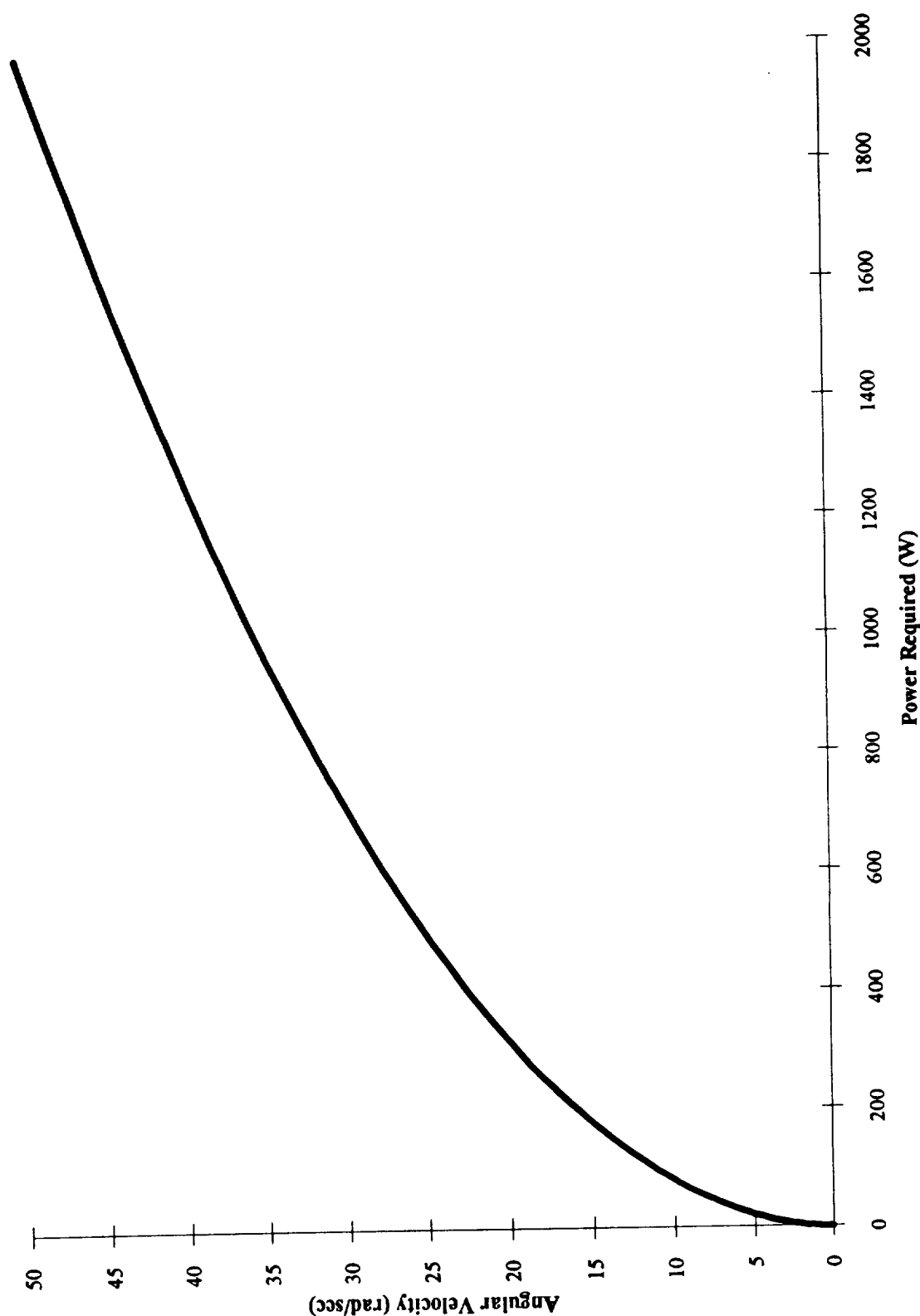
```
20
PRINT "You have run out of fuel mate"
60
CLS
PRINT USING "YOU FINISHED YOUR MISSION WITH #####.## Kg OF FUEL LEFT"; MF
PRINT ""
PRINT ""
PRINT "THANK YOU FOR USING THE MEDIUM DEBRIS COLLECTOR SPACECRAFT!!!"
END
```

**APPENDIX C**

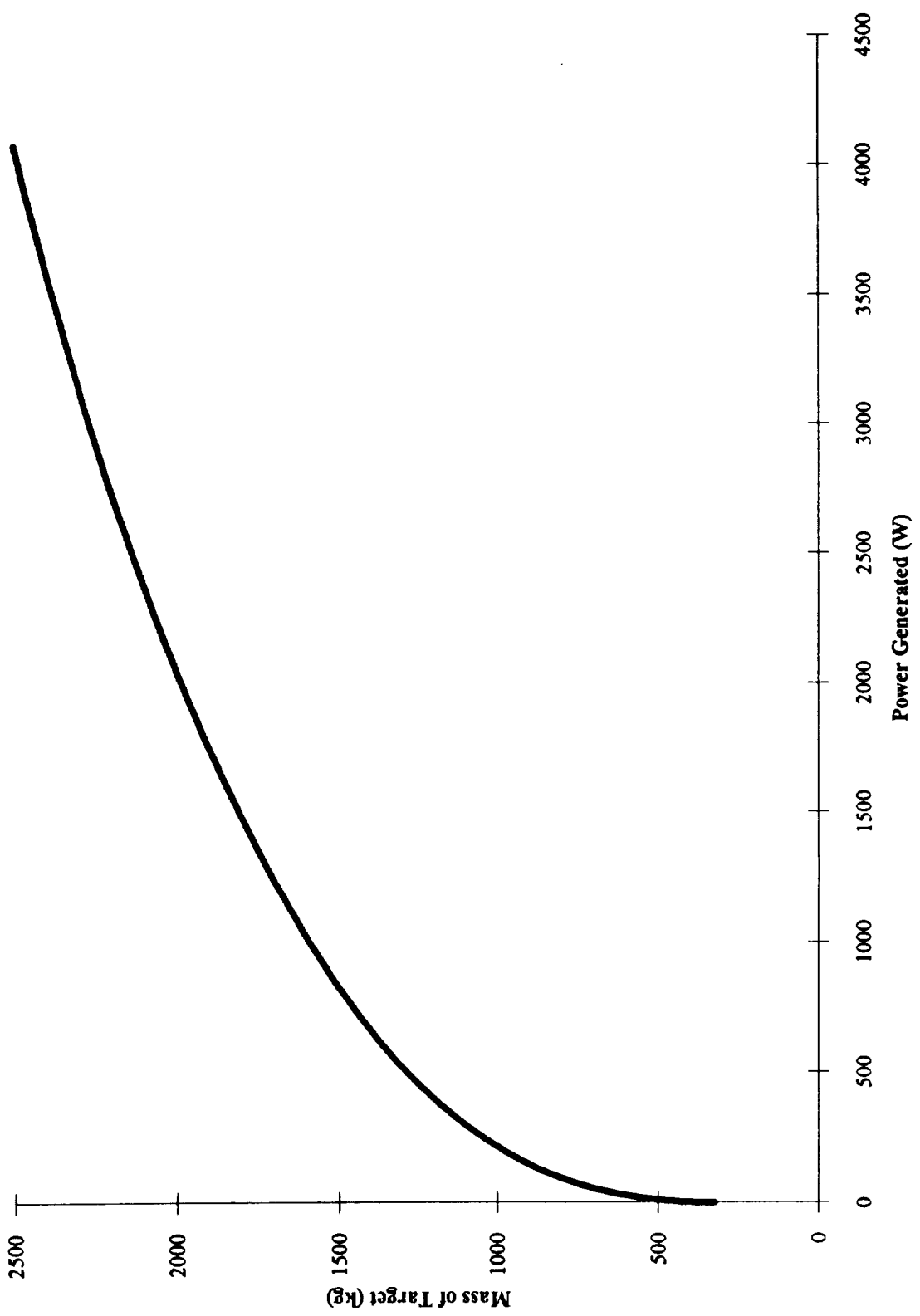


Spin Up Torques Versus Angular Accelerations





**Power Required Curve for Spin-Up Cycle**



**Power Generation Curve for Spin-Down Cycle**

Determination of End Effector Plate Size

A	B	C	D	E	F	G	H	I	J	K	L	M
Radius of largest object = 3 meters	Bea (inches)	Bea (inches)	Number of Segments	New number of segments (Using ratio approx 12.5%)	New Bea (inches)	New Bea (inches)	New diameter (inches)	Ratio of diameter	New Circumference (inches)		Diameter (inches)	Diameter (inches)
1	1.50	84.85	157.10	14.64	84.83	1.41	0.42	0.12	1.95		5.00	1.50
2	1.54	86.29	104.75	14.09	76.75	1.53	0.51	0.12	1.93			
3	1.57	87.73	74.50	9.97	71.00	1.75	0.60	0.12	1.90			
4	1.61	89.16	62.00	8.82	62.10	1.17	0.58	0.12	1.89			
5	1.65	90.59	52.47	7.97	52.54	1.06	0.58	0.12	1.91			
6	1.69	92.02	44.95	7.27	44.92	1.03	0.58	0.12	1.76			
7	1.73	93.45	38.43	6.69	38.41	0.94	0.54	0.11	1.69			
8	1.77	94.88	32.90	6.21	32.88	0.85	0.52	0.10	1.62			
9	1.81	96.31	28.37	5.81	28.35	0.77	0.49	0.09	1.54			
10	1.85	97.74	24.84	5.47	24.82	0.69	0.46	0.09	1.44			
11	1.89	99.17	21.31	5.18	21.29	0.64	0.44	0.09	1.34			
12	1.93	100.60	18.78	4.92	18.76	0.59	0.42	0.08	1.24			
13	1.97	102.03	16.25	4.68	16.23	0.54	0.40	0.07	1.14			
14	2.01	103.46	13.72	4.46	13.70	0.50	0.38	0.07	1.04			
15	2.05	104.89	11.19	4.25	11.17	0.46	0.36	0.06	0.94			
16	2.09	106.32	8.66	4.06	8.64	0.42	0.34	0.06	0.84			
17	2.13	107.75	6.13	3.89	6.11	0.39	0.32	0.05	0.74			
18	2.17	109.18	3.60	3.74	3.58	0.36	0.30	0.05	0.64			
19	2.21	110.61	1.07	3.60	1.01	0.33	0.28	0.05	0.54			
20	2.25	112.04	0.54	3.47	0.46	0.31	0.26	0.04	0.44			
21	2.29	113.47	0.41	3.35	0.39	0.29	0.24	0.04	0.34			
22	2.33	114.90	0.28	3.24	0.32	0.27	0.22	0.04	0.24			
23	2.37	116.33	0.15	3.14	0.25	0.25	0.20	0.03	0.14			
24	2.41	117.76	0.02	3.04	0.18	0.23	0.18	0.03	0.04			
25	2.45	119.19	0.00	2.94	0.11	0.21	0.16	0.03	0.00			
26	2.49	120.62	0.00	2.84	0.04	0.19	0.14	0.03	0.00			
27	2.53	122.05	0.00	2.74	0.00	0.17	0.12	0.03	0.00			
28	2.57	123.48	0.00	2.64	0.00	0.15	0.10	0.03	0.00			
29	2.61	124.91	0.00	2.54	0.00	0.13	0.08	0.03	0.00			
30	2.65	126.34	0.00	2.44	0.00	0.11	0.06	0.03	0.00			
31	2.69	127.77	0.00	2.34	0.00	0.09	0.04	0.03	0.00			
32	2.73	129.20	0.00	2.24	0.00	0.07	0.02	0.03	0.00			
33	2.77	130.63	0.00	2.14	0.00	0.05	0.00	0.03	0.00			
34	2.81	132.06	0.00	2.04	0.00	0.03	0.00	0.03	0.00			
35	2.85	133.49	0.00	1.94	0.00	0.01	0.00	0.03	0.00			
36	2.89	134.92	0.00	1.84	0.00	0.00	0.00	0.03	0.00			
37	2.93	136.35	0.00	1.74	0.00	0.00	0.00	0.03	0.00			
38	2.97	137.78	0.00	1.64	0.00	0.00	0.00	0.03	0.00			
39	3.01	139.21	0.00	1.54	0.00	0.00	0.00	0.03	0.00			
40	3.05	140.64	0.00	1.44	0.00	0.00	0.00	0.03	0.00			
41	3.09	142.07	0.00	1.34	0.00	0.00	0.00	0.03	0.00			
42	3.13	143.50	0.00	1.24	0.00	0.00	0.00	0.03	0.00			
43	3.17	144.93	0.00	1.14	0.00	0.00	0.00	0.03	0.00			
44	3.21	146.36	0.00	1.04	0.00	0.00	0.00	0.03	0.00			
45	3.25	147.79	0.00	0.94	0.00	0.00	0.00	0.03	0.00			
46	3.29	149.22	0.00	0.84	0.00	0.00	0.00	0.03	0.00			

ORIGINAL PAGE IS OF POOR QUALITY

## Appendix D1

```

/
=====Mesh Double Bumper=====
/
'This program calculates the thickness of the backwall for particles
'impacting the internal shield at 1 km/s (slow).
/
'input parameter
'=====
rhop = .05'g/cc
rhow = 2.78 'g/cc
sig = 35'ksi
cm = .45
v = 1'km/s
CLS
OPEN "A:\236\MDBrhSL.dat" FOR OUTPUT AS #1
'Calculation
'=====
pi = 4 * ATN(1#)
FOR rhop = .005 TO 3 STEP .05
FOR theta = 0 TO 60 * pi / 180 STEP 10 * pi / 180
FOR d = 10 TO 100 STEP 5
m = 4 / 3 * pi * (d / 2) ^ 3 * rhop 'particle mass
s = 30 * d
m1 = cm * d * rhop
m2 = .093 * d * rhop
mb = m1 + m2
mi = .06 * d * rhop
mw = 9 * m * v * COS(theta) / s ^ 1.5 * SQR(40 / sig)
tw = ((d * (COS(theta)) ^ (5 / 3) * (rhop) ^ .5 * v ^ (.666)) - .37 * (m
mw1 = 2.78 / 1000 * pi * (200) ^ 2 * tw
WRITE #1, d, theta * 180 / pi, rhop, tw, mw1
PRINT d, theta * 180 / pi, rhop, tw, mw1
NEXT d
PRINT
NEXT theta
NEXT rhop
CLOSE #1
END

```

## APPENDIX D2

```
'
=====Mesh Double Bumper=====
'input parameter
'=====
rhop = 2.78 'g/cc
rhow = 2.78 'g/cc
sig = 35'ksi
cm = .45
v = 10'km/s
CLS
OPEN "A:\236\MDBTWFA.dat" FOR OUTPUT AS #1
'Calculation
'=====
pi = 4 * ATN(1#)
FOR d = .1 TO 1.1 STEP .1
theta = 45 * pi / 180
m = 4 / 3 * pi * (d / 2) ^ 3 * rhop 'particle mass
s = 30 * d
m1 = cm * d * rhop
m2 = .093 * d * rhop
mb = m1 + m2
mi = .06 * d * rhop
mw = 9 * m * v * COS(theta) / s ^ 1.5 * SQR(40 / sig)
tw = mw / rhow
mt = mw + mb + mi
PRINT d, theta * 180 / pi, tw, mt
WRITE #1, d, theta * 180 / pi, tw, mt
NEXT d
CLOSE #1
END
```

## APPENDIX D3

## Multi-Shock Shield

```
'
'***** Multi-Shock Shield *****
```

```
' Input Parameters
```

```
'-----
```

```
rhop = 2.78 'g/cc
sig = 35 'ksi
rhow = 2.78 'g/cc
pi = 3.14159
```

```
OPEN "A:\mulskext.dat" FOR OUTPUT AS #1
```

```
'Calculated Parameters
```

```
'-----
```

```
'Input expected values for incidence angle and velocity
```

```
theta = 45 * pi / 180
v = 10
```

```
'Vary the diameter of the particle and calculate the back wall thickness
```

```
FOR d = .1 TO 1.1 STEP .1
```

```
  s = 30 * d
  m = rhop * 4 / 3 * pi * (d / 2) ^ 3
  mb = .19 * d * rhop
  vn = v * (COS(theta))
  mw = 41.7 * m * (vn / (s ^ 2)) * (40 / sig) ^ .5
  tw = mw / rhow
  WRITE #1, d, tw
```

```
NEXT d
END
```

```

/
/*****          APPENDIX D4          *****/
/*****          INTERNAL Multi-Shock Shield          *****/
/*****          density of impinging particle tests          *****/

/ Input Parameters
/-----

sig = 35 'ksi
rhow = 2.78 'g/cc
pi = 3.14159

OPEN "A:\mulskden.dat" FOR OUTPUT AS #1

/Calculated Parameters
/-----

/ Input expected values for incidence angle , particle diameter, and velocity

theta = 45 * pi / 180 'radians
v = 1 'km/s
d = .5 'cm
/Vary the density of the particle and calculate the back wall thickness

FOR rhop = .0005 TO 3 STEP .0005
  s = 30 * d
  m = rhop * 4 / 3 * pi * (d / 2) ^ 3
  mb = .19 * d * rhop
  vn = v * (COS(theta))
  mw = 41.7 * m * (vn / (s ^ 2)) * (40 / sig) ^ .5
  tw = mw / rhow
  WRITE #1, rhop, tw
NEXT rhop
END

```

APENDIX D5

\*\*\*\*\* INTERNAL Multi-Shock Shield \*\*\*\*\*

' Input Parameters

'-----  
 rhop = .05 'g/cc  
 sig = 35 'ksi  
 rhow = 2.78 'g/cc  
 pi = 3.14159

OPEN "A:\mulskint.dat" FOR OUTPUT AS #1

'Calculated Parameters

'-----  
 fifty = 50 \* pi / 180

' Vary the incidence angle and diameter of the particle,  
 ' and calculate the back wall thickness

```
FOR theta = 0 TO fifty STEP (10 * pi / 180)
  FOR d = 10 TO 100 STEP 5
    s = 30 * d
    m = rhop * 4 / 3 * pi * (d / 2) ^ 3
    mb = .19 * d * rhop
    v = 1
    vn = v * (COS(theta))
    mw = 41.7 * m * (vn / (s ^ 2)) * (40 / sig) ^ .5
    tw = (SQR(sig / 40) * (COS(theta)) ^ (4 / 3) * SQR(rhop) * v ^ (2 / 3)) *
    WRITE #1, d, tw
  NEXT d
NEXT theta
END
```